GUSTAVO ANTONIO CORREA MOMESSO

MINIPLATES COATED BY PLASMA ELECTROLYTIC OXIDATION IMPROVE BONE HEALING OF SIMULATED FEMORAL FRACTURES ON LOW BONE MINERAL DENSITY RATS

Araçatuba – SP
2020

GUSTAVO ANTONIO CORREA MOMESSO

MINIPLATES COATED BY PLASMA ELECTROLYTIC OXIDATION IMPROVE BONE HEALING OF SIMULATED FEMORAL FRACTURES ON LOW BONE MINERAL DENSITY RATS

Tese apresentada à Faculdade de Odontologia do Campus de Araçatuba – Universidade Estadual Paulista "Júlio de Mesquita Filho"- UNESP, para obtenção do Título de Doutor em Odontologia (Área de concentração em Cirurgia e Traumatologia Bucomaxilofacial)

Orientador: Prof. Ass. Dr. Leonardo Perez Faverani
Coorientadora: Profª. Associada. Drª. Roberta Okamoto

Araçatuba – SP
2020

Catalogação na Publicação (CIP)

Diretoria Técnica de Biblioteca e Documentação – FOA / UNESP

M732m

Momesso, Gustavo Antonio Correa.

Miniplates coated by plasma electrolytic oxidation improve bone healing of simulated femoral fractures on low bone mineral density rats / Gustavo Antonio Correa Momesso. - Araçatuba, 2020

62 f. : il. ; tab.

Tese (Doutorado) – Universidade Estadual Paulista, Faculdade de Odontologia de Araçatuba

Orientador: Prof. Leonardo Perez Faverani

Coorientadora: Profa. Roberta Okamoto

1. Osteoporose 2. Ovariectomia 3. Fraturas ósseas 4. Fixação interna de fraturas I. T.

Black D7

CDD 617.64

Claudio Hideo Matsumoto – CRB-8/5550

Dedicatória

Dedico este trabalho às pessoas mais importantes de minha vida:

Ao meu amado pai, **Idanir Antonio Momesso Junior,** fonte de amor infindável. Infelizmente, o destino nos distanciou para que eu pudesse cumprir esta longa jornada. São 10 anos que este trajeto se iniciou e, apesar da saudade imensurável e as dificuldades aqui enfrentadas, a conquista de hoje remete à maneira preciosa que dedicastes sua vida inteira pelos seus filhos. Apesar de um dia memorável e que representa uma conquista para todos nós, o maior legado que você me deixou não está nesses papéis. Este árduo e impetuoso caminho só poderia ser concretizado com sucesso através dos valores morais que me foram passados durante toda minha criação. A minha maior felicidade hoje é poder me orgulhar da pessoa que me tornei, com caráter, ética e altruísmo, valores inestimáveis e que permanecem para a eternidade. Todos os dias quando acordo peço a Deus que me dê forças para poder sempre dar meu melhor e fazer o bem. Somente essa herança foi capaz de me fazer chegar onde estou obtendo o sucesso que obtive. Ser pai é muito mais do que financiar um projeto de vida desses que estamos concretizando. É formar um ser humano através dos seus princípios. O seu papel foi cumprido com excelência, pois poucas pessoas são capazes e perfazê-lo.

A minha amada mãe, **Maria Luiza Correa Momesso**, a quem dedico todo meu amor. Mãe, a senhora participou de todos os momentos de minha vida e esteve presente em todos os pequenos detalhes. Acompanhou todo o meu trajeto, desde meu início de vida escolar até os dias em que estava vivendo a grande ansiedade do vestibular. É impossível transcrever e agradecer toda sua dedicação e amor para com seus filhos. Sem isso, seria impossível transcender estas etapas. Sua participação nesta conquista é fundamental e meu agradecimento e amor por você, é eterno!

Ao meu irmão, **Idanir Antonio Momesso Neto**, por ser meu melhor amigo, em todos os momentos. Temos histórias de vida parecidas. Saímos cedo de casa para realizarmos nossos sonhos. Sempre tive em você minha grande inspiração e referência em minha vida. É notório o amor imensurável que tens pela sua família e toda sua dedicação para com ela e *"um homem que não se dedica à família jamais será um homem de verdade"*. Com certeza, você tornou este percurso mais fácil e é impossível transcrever sua importância nele. Sou eternamente

grato pelo seu companheirismo, amor e por ser esta pessoa a quem considero muito mais que um irmão. Te amo eternamente!

A minha irmã, **Marília Gabriela Correa Momesso,** por todo o apoio e amparo que sempre que me deu, desde meus tempos de colegial me incentivando e ajudando com os estudos, tornando-se uma grande referência em minha vida. Ter a mesma profissão que você é uma grande responsabilidade que carrego por toda sua competência e inteligência. Ao mesmo tempo, tudo se torna mais fácil pelo exemplo que tenho ao meu lado. Obrigado por todo carinho, amor e zelo que sempre teve por mim, como irmão mais novo. Você fez parte de toda minha formação como ser humano. Este título tem parte fundamental sua. Te amo para sempre!

Agradecimentos especiais

AGRADECIMENTOS ESPECIAIS

A Deus, por ser uma pessoa privilegiada. Alguns momentos de dificuldades em nossas vidas nos deparamos sozinhos. Esta longa jornada, cheia de intempéries e frustrações só poderia ser suportada com o amparo da força maior. O sentimento de proteção, zelo e amor que sentimos com a presença de Deus é que nos fortalece e impulsiona a seguir em frente diante de todas as barreiras impostas a nós. Obrigado, meu Deus, por nunca me abandonar nos momentos que mais precisei, ainda que tivesse todos os motivos para isso.

Ao meu querido Orientador e amigo, **Prof. Ass. Dr. Leonardo Perez Faverani**. Minha admiração pelo profissional e pessoa incrível que és iniciou ainda enquanto graduando, durante o período do seu doutorado. Tenho guardado em minha memória e coração todos os bons momentos que passamos juntos, durante todos esses anos. Agradeço imensamente a Deus por me proporcionar estar ao lado de pessoas boas, especiais e leais como você. Sem dúvidas, lhe devo muito pela amizade que construímos ao longo desses cinco anos e espero que possamos manter isso sempre vivo. Citar as qualidades como Cirurgião, Pesquisador e Professor inerentes a você, torna-se pleonasmo e acredito que estas devem e sempre lhe serão creditadas, pois representas um ponto fora da curva, como profissional. Tudo que aprendi neste percurso devo ao dom que Deus lhe deu do ensino e se sou quem sou hoje, profissionalmente, devo a você e serei eternamente grato. Sempre digo que todos deveriam ter a oportunidade de conhecê-lo, pela sua bela história de vida e pela pessoa que és: determinado, gênio, carismático altruísta, sensitivo, sempre disposto ajudar todos ao redor, além de o senso de justiça aguçado. Você sempre tem muito a acrescentar na vida das pessoas e amizades como a sua são raras e devem ser regadas e eternizadas. Tenho muito orgulho de ter acompanhado de perto e, de alguma maneira, participado de todo seu trajeto e ascensão desde o contrato nesta universidade. O seu caminho é, sem dúvidas, o mais belo possível e muitas coisas boas hão de acontecer em sua vida profissional e pessoal. Lembre-se que mesmo nos momentos de maior fragilidade, dúvidas e sensações de injustiças, Deus está conosco, pois ele nunca dorme.

Ao **Prof. Associado Osvaldo Magro-Filho** por aceitar de prontidão compor a banca examinadora deste grande dia de conclusão de doutorado. Professor, agradeço muito pela

ótima convivência e recepção que sempre tem conosco da pós-graduação. Tenho profunda admiração pelo grande profissional e ser humano que és. Grande Cirurgião e Professor, do qual tenho imenso orgulho de ter sido aluno e o qual sempre serei. Tê-lo neste dia tão especial traz grande responsabilidade, mas também muita honra.

Ao **Prof. Associado. Eduardo Hochuli Vieira** por aceitar compor e ilustrar a banca examinadora. Professor, é uma grande honra recebê-lo para avaliar nosso trabalho. Nutro grande admiração pelo senhor e tenho muito orgulho em poder dizer que fez parte, ainda que indiretamente, da minha formação como Cirurgião e Professor. Um dos maiores nomes e grande representante da Cirurgia Buco-Maxilo-Facial do Brasil. Todos da área só temos a agradecer pelo trabalho impecável que exerce em nossa atuação. Tenho certeza de que és grande inspiração para todos os cirurgiões em formação e mesmo os profissionais atuantes.

Ao **Prof. Associado. Jamil Awad Shibli** por aceitar compor esta banca examinadora, apesar dos inúmeros compromissos e agenda disputada. É um grande orgulho e honra ter um nome tão importante quanto o do senhor nesta data. Tenho profunda admiração pelo grande Pesquisador, Cirurgião-Dentista e empreendedor que és. Fonte de inspiração a muitos profissionais do mundo todo.

Ao **Prof. Associado. Valentim Adelino Ricardo Barão** pelo aceite em compor esta banca examinadora e, principalmente, por ter papel fundamental na execução deste projeto. Professor, o senhor é um grande exemplo de pesquisador para todos os jovens que estão ingressando na área acadêmica. Sem dúvidas, o senhor é um grande fenômeno da odontologia brasileira, o qual coleciona conquistas grandiosas e meritórias ainda que tão jovem. Fonte de inspiração como profissional e orientador. Agradeço toda ajuda incessante que nos proporcionou durante o período de doutoramento. Tenho gratidão eterna por toda valiosa contribuição.

A minha querida coorientadora **Profa. Associada Roberta Okamoto** por ter sido minha orientadora durante o mestrado e me passado tantos conhecimentos sobre a arte da docência. A senhora é um grande exemplo de pesquisadora e docente que inspira todos ao seu redor.

Aos Professores da Disciplina da Cirurgia e Traumatologia Bucomaxilofacial **Dr. Idelmo Rangel Garcia-Júnior, Alessandra Marcondes Aranega, Daniela Ponzoni, Ana Paula Farnezi Bassi, Francisley Ávila Souza e ao ilustríssimo Professor Tetuo Okamoto (*in*

***memoriam*)**, pelo carinho, coleguismo, auxílio, exemplo e amizade desfrutada em nosso departamento. Recebam o meu carinho e admiração.

Aos **Professores Valdir Gouveia Garcia** e **Letícia Helena Theodoro**, recebam toda minha gratidão. Dificilmente encontramos em nossas vidas pessoas tão especiais quanto vocês. É impressionante a humildade que carregam apesar de serem grande expoentes da nossa odontologia e da periodontia mundial. Não há atitudes, palavras ou gestos que possam retribuir todas as oportunidades e conhecimento que me passaram durante minha pós-graduação, incluindo a possibilidade de participar em um capítulo do livro que idealizaram e de extrema importância para a odontologia. Com certeza será um marco. Tenho orgulho e honra de poder dizer que foram meus mestres e hoje são também grandes amigos.

À Cecília Alves de Sousa. Você é, sem dúvidas, a pessoa mais importante para mim nesta trajetória toda. Acompanhamos os passos um do outro desde o início de tudo. Crescemos, acertamos e erramos juntos. Nos mantivemos firmes e fortes frente a todas adversidades e, assim como eu, você está atingindo o fim desta árdua trajetória acadêmica. Não é fácil lidar com as próprias intempéries inerentes ao processo de pós-graduação, ainda mais desafiador é lidar com as dificuldades de outrem. Acredito que conseguimos nos apoiar sempre em todos os momentos e isso é imprescindível para que o sucesso de tudo isso seja alcançado. Sou eternamente grato por tudo que vivemos e após este longo percurso, com certeza me tornei uma pessoa melhor por nossa convivência. O seu sucesso é mais do que sacramentado e cada dia que passa me impressiono mais e mais descobrindo o quão capaz você é ao desenvolver qualquer atividade que se propõe. Por mais que as incertezas que a vida nos impõe sejam grandes, tenha certeza de que seu futuro só lhe reserva acontecimentos extraordinários e pode contar comigo sempre que precisar. Permaneça sempre essa pessoa com bom coração, altruísta, de caráter ilibado.

Ao meu grande amigo **Valthierre Nunes de Lima**, eterno companheiro. Meu amigo, tenho muita gratidão em ter lhe conhecido. Espero levar essa nossa amizade para eternidade. Você foi um grande irmão para mim durante o período de pós-graduação. Sua amizade agregou muitas coisas boas em minha vida. Aprendi e aprendo muito com você. Amizades verdadeiras e honestas como a sua são raridade e, apesar de não estarmos mais tão próximos, desejo que isso permaneça. Você é um ser humano ímpar, daqueles que poucas vezes cruzamos durante a vida. Lhe admiro como grande cirurgião, professor e profissional que és. Mas lhe admiro mais ainda pela pessoa que é com todos a sua volta. Sinto bastante falta de ter um parceiro para

todas as horas, mas sinto-me muito satisfeito e feliz em ver o seu processo de crescimento e evolução. Você é um sucesso declarado.

Ao meu grande amigo **Tárik Ocon Braga Polo**. Grande irmão que Araçatuba me trouxe. Sempre conto a história de quando lhe conheci, em uma carona do campus da faculdade para a cidade. Ainda graduando, dentro do seu "carrinho", fomos discutindo um pouco sobre traçar o caminho cirúrgico durante a graduação. Você já era um estagiário importante na cirurgia e eu almejava este lugar. Cá estamos nós, você Doutor e eu próximo deste título tão importante. Obrigado pela amizade e companheirismo de sempre, nos bons momentos, "tomando uma" para relaxar e nos momentos difíceis de árduo trabalho, nos quais você esteve sempre disponível para qualquer situação. Agradeço a Deus por colocar sempre boas pessoas em minha vida e você é uma delas, um amigo e um irmão muito especial e que levarei para o resto da vida, com certeza.

Ao grande amigo **William Phillip Pereira da Silva**. Obrigado pela amizade sincera e pela ótima convivência em momentos nem sempre tão agradáveis. Muito bom poder dividir esta amizade durante este período difícil. Grande parceiro dos chopps artesanais, noites de muito blues, Mutum Cavalo e compartilhamentos de problemas que não são poucos os quais passamos durante a pós-graduação. Lhe admiro muito como cirurgião e profissional. Tenho certeza de que seu caminho será repleto de sucesso e torço para que nunca percamos a amizade que construímos.

Ao grande amigo **Tiburtino José de Lima Neto.** Obrigado por agregar tanto com a sua chegada. Sem dúvidas sua chegada ao grupo foi um grande acréscimo e tenho certeza de que tens um futuro brilhante como cirurgião e pós graduando, futuro professor. Permaneça sempre essa pessoa com um bom coração que está sempre disposto a ajudar a todos.

Ao grande amigo **Anderson Maikon de Souza Santos.** Grande amigo que fiz na pós-graduação. Desde o início me identifiquei bastante com sua pessoa, meu amigo. Desde as ideias políticas até os gostos musicais e filmes. Muito feliz em poder concretizar uma nova amizade durante este percurso, logo no seu fim, mas que perdurará por muito tempo, com toda a certeza. Você é um grande profissional e cirurgião e está sempre disposto a ajudar em qualquer momento. Seu sucesso é mais do que garantido e iremos nos encontrar nos COBRACS da vida daqui 15 anos.

Ao grande amigo **Leonardo Alan Delanora.** Obrigado pela amizade construída, apesar do pouco tempo de convivência. Grande parceiro de música, puro malte e de discussões sobre o mercado financeiro. Tenho muito apreço por ti e pela nossa amizade. Espero que possamos continuar a nutrindo por muitos anos.

A minha querida amiga **Barbara Rios,** a mais nova integrante do grupo do **Professor Leo.** **"**Bá", sempre tive muito apreço pela pessoa que você é; humilde, esforçada e inteligente. Mas confesso que tive uma grata surpresa lhe conhecendo mais. Tens agregado muito ao grupo e, com certeza, é uma pós graduanda que extremamente competente e que tem trabalhado arduamente. O seu futuro é de sucesso, sem dúvidas e agradeço muito pela sua valiosa parceria e amizade que foi muito importante para mim neste ano.

Aos amigos da "velha guarda" **Erik Neiva, Leonardo da Silva, João Paulo Bonardi e Ciro Borges Duailibe**. Tenho muito orgulho da turma que formamos e sou muito grato a amizade que construímos. Espero, de verdade, levar essa relíquia para toda a vida. Obrigado por contribuírem de maneira indireta e direta para a conclusão da minha formação.

Aos **alunos de iniciação científica**, pela disponibilidade e ajuda imprescindível que exercem na realização de todos os projetos. Sem o comprometimento e força de vontade de vocês, nada disso seria possível. Em especial aos alunos **João Matheus Fonseca e Santos e Stefany Barbosa** que estiveram conosco desde o início da idealização deste trabalho e se comprometeram de maneira excepcional para que tudo ocorresse de maneira perfeita. Vocês são incríveis e têm um futuro brilhante pela frente.

À Coordenação de Aperfeiçoamento Pessoal de Nível Superior (CAPES). O presente trabalho foi realizado com apoio da Coordenação de Aperfeiçoamento de Pessoal de Nível Superior – Brasil (CAPES) – Código de financiamento 001.

À Fundação de Amparo à Pesquisa do Estado de São Paulo (FAPESP), pela concessão do auxílio pesquisa regular Processo nº 2016/20297-6, em nome do pesquisador **Leonardo Perez Faverani** que fomentou parte desta pesquisa.

Ao **Laboratório de caracterização e avaliação de resposta biológica,** na pessoa do **Prof. Dr. Élcio Marcantônio Júnior e à Técnica de laboratório Ana Cláudia Gregolin Costa Miranda**, da Faculdade de Odontologia de Araraquara – UNESP, pela utilização do EXAKT para cortes de peças calcificadas.

Ao **laboratório de plasmas tecnológicos,** na pessoa do **Prof. Nilson Cristino Cruz** pela facilitação da texturização de superfície das placas por PEO e pela caracterização de superfície das placas.

Ao **"Bone Research Lab",** da Faculdade de Odontologia de Ribeirão Preto – USP, na pessoa do **Prof**. **Adalberto Luiz Rosa e aos Pós-doutorandos Gileade P. Freitas e Helena Bacha Lopes,** pela facilitação das análises de biologia molecular por PCR.

Ao **laboratório de Prótese Total** da Faculdade de Odontologia de Piracicaba - UNICAMP**,** na pessoa do **Prof. Valentim Adelino Ricardo Barão e demais integrantes** por todo apoio e ajuda, ademais pelo fornecimento de materiais para que fosse possível a realização da texturização de superfície das placas.

À empresa **ENGIMPLAN,** na pessoa do **Sr. José Tadeu Leme** por ter cedido todas as miniplacas e parafusos usados nesta pesquisa, fazendo este projeto virar realidade.

Agradecimentos

AGRADECIMENTOS

À Faculdade de Odontologia de Araçatuba – UNESP, na pessoa do diretor **Prof. Tit. Glauco Issamu Miyahara** pela oportunidade de realização dos cursos de Graduação e Mestrado. Devo tudo que conquistei, principalmente, a esta universidade que me proporcionou os melhores ensinamentos, professores e estrutura que poderia ter. Sou eternamente grato à FOA-UNESP.

Ao **Programa de Pós-Graduação em Odontologia**, da Faculdade de Odontologia de Araçatuba, da Universidade Estadual Paulista "Júlio de Mesquita Filho" com o atual Coordenador **Prof. Adj. André Luiz Fraga Briso.**

Aos **funcionários da Pós-graduação da Faculdade de Odontologia de Araçatuba - UNESP** pela disponibilidade e paciência em todas as etapas do doutorado. Pelo trabalho honesto e sempre ágil.

Aos **funcionários da Biblioteca da Faculdade de Odontologia de Araçatuba – UNESP** pela prontidão em nos atender e carinho.

Aos **funcionários do Departamento de Cirurgia e Clínica Integrada (Paulo Gratão, Renato e Marco).** Muito obrigado pelo carinho e respeito.

Aos colegas da pós-graduação da área de Cirurgia e Traumatologia Bucomaxilofacial Aprendi muito a cada momento com cada um de vocês. Obrigado pelo auxílio constante na minha vida e na pós-graduação.

Aos **pacientes**, pela credibilidade e confiança depositadas a nós pós-graduandos, premitindo-nos aprimorar as habilidades cirúrgicas e, como sempre estaremos em nossas vidas, aprendendo constantemente. Minha eterna gratidão.

Não é o cérebro que mais importa, mas sim o que o orienta: o caráter, o coração, a generosidade, as ideias progressivas

(Fiódor Dostoiévski)

Momesso GAC. Miniplacas texturizadas pela oxidação por plasma eletrolítico melhoram o reparo ósseo em simulações de fraturas femorais de ratas com baixa densidade mineral óssea [tese]. Aracatuba: Faculdade de Odontologia, Universidade Estadual Paulista (Unesp); 2020.

RESUMO

O tratamento de pacientes politraumatizados representa um grande desafio nas áreas de cirurgia maxilofacial e ortopédica. Portanto, este estudo testou a hipótese de que o uso de um revestimento bioativo (por oxidação eletrolítica de plasma, PEO) em microplacas de titânio poderia melhorar a cicatrização de fraturas de ratos com baixa densidade mineral óssea (DMO). Trinta ratas foram submetidas à cirurgia de ovariectomia bilateral (OVX) e 35 ratas foram submetidas à cirurgia falsa (SHAM). Três meses depois, os animais foram submetidos à simulação de fratura do fêmur, os quais foram fixados com miniplacas de titânio não revestidas (CONV) ou revestidas (PEO). Oito semanas de pós-operatório, os complexos miniplaca/osso foram analisados por meio de microtomografia computadorizada, histometria, microscopia confocal, análise molecular e biomecânica. Elementos bioativos (Ca e P) foram incorporados na miniplaca revestida por PEO e a superfície foi modificada em uma estrutura semelhante a um vulcão. Na análise microCT, o grupo OVX / PEO apresentou maiores valores para os parâmetros Tb.Th (espessura trabecular óssea), Tb.Sp (separação das trabéculas ósseas) e Tb.N (número de trabéculas) em comparação com o grupo OVX / CONV. De acordo com a análise histométrica, o grupo OVX / PEO apresentou formação de osso novo significativamente maior do que o grupo OVX / CONV ($P < 0,05$). Para a área de fluorocromo, os grupos OVX (PEO e CONV) apresentaram maiores valores de precipitação de calceína (osso velho) do que vermelho de alizarina (osso novo). Os resultados moleculares mostraram maiores valores para proteínas relacionadas à fase final de formação óssea ($P < 0,05$) no grupo OVX / PEO. O grupo OVX / PEO apresentou maior resiliência do sistema de osso / miniplaca em comparação com os demais ($P < 0,05$). Concluiu-se que o revestimento PEO otimiza a consolidação óssea em fraturas femorais simuladas em ratos com baixa densidade mineral óssea. Isso lança uma nova luz no tratamento de pacientes osteoporóticos com fraturas ósseas.

Palavras-chave: Osteoporose. Ovariectomia. Fraturas ósseas. Fixação interna de fraturas.

Momesso GAC. Miniplates coated by plasma electrolytic oxidation improve bone healing of simulated femoral fractures on low bone mineral density [tese]. Aracatuba: Faculdade de Odontologia, Universidade Estadual Paulista (Unesp); 2020.

ABSTRACT

The treatment of polytrauma patients represents a great challenge in the maxillofacial and orthopedic surgery fields. Therefore, this study tested the hypothesis that the use of a bioactive coating (by plasma electrolytic oxidation, PEO) on titanium microplates could improve the fracture healing of low bone mineral density (BMD) rats. Thirty female rats underwent bilateral ovariectomy surgery (OVX), and 35 rats underwent fake surgery (SHAM). Three months later, animals were subjected to femoral fracture simulation and were fixed with either non-coated (CONV) or coated (PEO) titanium miniplates. Eight weeks postoperatively, microplate/bone complexes were analyzed through computed microtomography, histometric, confocal microscopy, molecular, and biomechanical analysis. Bioactive elements (Ca and P) were incorporated on the PEO microplate and the surface was modified in a volcano-like structure. In the microCT analysis the OVX/PEO group had greater values for Tb.Th (bone trabecular thickness), Tb.Sp (separation of bone trabeculae) and Tb.N (number of trabeculae) parameters compared to the OVX/CONV group. According to histometric analysis, the OVX/PEO group showed significantly higher new bone formation than the OVX/CONV group ($P < 0.05$). For the fluorochrome area, the OVX groups (PEO and CONV) showed greater values for calcein precipitation (old bone) than alizarin red (new bone). Molecular results showed greater values for proteins related to the final phase of bone formation ($P < 0.05$) in the OVX/PEO group. The OVX/PEO group showed higher bone/miniplate system resilience compared to the others ($P < 0.05$). It was concluded that PEO coating optimizes bone healing on simulated femoral fractures in low bone mineral density rats. This sheds new light in the treatment of osteoporotic patients with bone fractures.

Keywords: Osteoporosis. Ovariectomy. Bone fractures. Fracture fixation, internal.

Listas

LISTA DE TABELAS

Table 1 Mechanical data of femur bone from OVX and SHAM groups. Data are expressed as mean ±standard deviation. 43

LISTA DE FIGURAS

Figure 1	Experimental design and timeline regarding to osteoporosis induction; fracture simulation and osteosynthesis; administration of fluorochromes of decalcified group and euthanasia.	31
Figure 2	Stages of the ovariectomy surgical procedure. (A) Incision on the flanks of rats; (B) Divulsion of the subcutaneous anatomical planes; (C) Access to the peritoneum; (D) Incision of the peritoneum and access to the abdominal cavity; (E) Location of the ovary and uterine horn; (F) Tubal ligation of the uterine horn; (G) Ovary removed; (H) Replacement of lacquered fabrics; (I) Suturing the internal planes; (J) Suture of the superficial plane.	32
Figure 3	Biomechanical test for osteoporosis validation. (A) Tibia positioned and stabilized by an anterior and posterior support, preventing it to move and (B) Application of vertical force in the central region of the femur, at a load rate of 5mm / min.	33
Figure 4	Stages of the surgical procedure to simulate femoral fractures. (A) 4 cm incision in the lateral femoral region; (B) Visualization of the lateral muscle and biceps of the femur; (C) Exposure of the lateral pole of the femoral condyle; (D) Fixing the 1.5 mm titanium miniplate system with four screws and without intermediary; (E) 1mm osteotomy in the epiphyseal metaphysis with circular metal disc to simulate femur fracture; (F) Final aspect of the osteotomy.	34
Figure 5	Procedures for analysis by computed microtomography. (A) SkyScan microtomography device; (B) Femures positioned and stabilized by acrylic resin on the microtomography device; (C) Image obtained by scanning; (D) Reconstructions of microtomographic images.	36
Figure 6	(A) Sample of fixed femur after reduction and inclusion on TechnoVit® resin mounted on histological blade. (B) Blades obtained after the Exakt cutting until 100 μm thick. (C) Region of interest (ROI) between the two most proximal screws and the first third bone/plate complex.	38

Figure 7 Procedures for Biomechanical test for bone / miniplates complex. (A) Inclusion of femurs in acrylic resin; (B) Femoral stabilized on the DL 3000 universal machine for testing; (C) Load cell model used for load application. 40

Figure 8 Images of the as-received non-coated titanium miniplate for internal fixation (CONV) and PEO-coated titanium miniplate (top images). Representative micrographs of scanning electron microscopy in the magnitudes of 300× and 2000× of CONV and PEO-coated miniplates (middle images). Color figures show the chemical mapping of microplate surfaces by EDS with element concentration (wt%) (Ti, O, Ca and P). 42

Figure 9 Laser confocal microscopy photomicrographs of the slides (10× magnification) (bottom figures). The green color represents fluorochrome calcein (old bone), and the red color represents precipitation of alizarin (new bone). Bar = 100 μm. 44

Figure 10 Quantitative area (in μm2) of calcein and alizarin fluorochromes (top image). The statistical difference between groups is showed with the p-value in the figure. Data are expressed as mean ± standard deviation. 44

Figure 11 Gene expression by real-time PCR of RUNX-2 (runt-related transcription factor 2), BMP-2 (bone morphogenetic protein 2), Osterix, ALP (alkaline phosphatase), COL-1 (collagen 1) and Osteocalcin. The statistical difference between groups is showed with the p-value in the figure. Data are expressed as mean ± standard deviation. 45

Figure 12 Photomicrographs of histological slides stained with Stevenel blue and alizarin red (25× magnification), showing a great aspect of new bone formation during femoral healing of OVX/PEO and little presence of adipose and connective tissue. The OVX/CONV group showed few areas of new bone formation and significant presence of adipose and connective tissue. BT – bone tissue; CT – connective tissue. Bar = 100 μm. 46

Figure 13 New bone formation (in %) evaluated by histometric analysis. The statistical difference between groups is showed with the p-value in the figure. Data are expressed as mean ± standard deviation. 46

Figure 14 Bone formation parameters obtained through computed microtomography. (a) Percent bone volume (BV.TV) (unit: %) (b) Trabecular thickness (Tb.Th) (unit: mm2). (c) Trabecular number (Tb.N) (unit: total number). (d) Trabecular space (Tb.Sp) (unit: mm3). The statistical difference between groups is showed with the p-value in the figure. Data are expressed as mean ± standard deviation. 47

Figure 15 Bone resilience (in mJ) values obtained in the biomechanical test by 3 points flexion. The statistical difference between groups is showed with the p-value in the figure. Data are expressed as mean ± standard deviation. 48

Figure 16 Photomicrographs (40× magnification) from organs (brain, heart, kidney, liver, lungs, and skeletal striated muscle) to observe the presence of possible contamination by metal ions from the microplates. Bar = 10 μm. 49

LISTA DE ABREVIATURAS

µm	Micrometers
ALP	Alkaline phosphatase
BMD	Bone mineral density
BMP2	bone morphogenetic protein
BV/TV	Bone volume percent
COL1	colagen 1
CONV	Conventional coating
DC	Direct current
EDS	Energy dispersive spectroscopy
FDA	Food and Drug Administration
HE	hematoxylin and eosin
M	Molar
mg/kg	Miligram per kilogram
mL	Mililiters
mm	Milímeters
NBF	New bone formation
OC	osteocalcin
OSX	osterix
OVX	Ovariectomy
p	Unit of statistical relevance
PCR	C-reactive protein
PEO	Plasma Electrolytic Oxidation
Po.Tot	Total porosity
ROI	Region of interest
RUNX -2	runt-related transcription factor
SEM	Scanning electron microscopy
SHAM	Fake surgery
Tb.N	Trabecular number
Tb.Sp	Trabecular space
Tb.Th	Trabecular thickness
uL	Microliters

SUMÁRIO

1 INTRODUCTION 26
2 METHODS 29
3 RESULTS 42
4 DISCUSSION 51
REFERENCES 56
ANEXOS 61

Miniplates coated by plasma electrolytic oxidation improve bone healing of simulated femoral fractures on low bone mineral density[*]

(Miniplacas texturizadas pela oxidação por plasma eletrolítico melhoram o reparo ósseo em simulações de fraturas femorais de ratas com baixa densidade mineral óssea)

[*] *Este trabalho foi formatado de acordo com as normas do periódico Biomaterials (https://www.elsevier.com/journals/biomaterials/0142-9612?generatepdf=true)*

Introduction

1 INTRODUCTION

The ultimate treatment of ill polytrauma patients represents a great challenge in the maxillofacial and orthopedic surgery fields. Internal fixation is the current treatment employed and shows a great success rate in clinical practice, mainly in healthy patients with no systemic disorders [1, 2]. However, the treatment success and mitigation of sequels are dependent on the mechanical stability, bone healing, biomaterial quality, and systemic metabolism.

In this context, low bone mineral density (BMD), comminuted fractures, and severe unfavorable fractures could interfere with the fracture healing [3, 4]. Osteoporosis is the most common condition related to low BMD, and osteoporotic patients are the most susceptible to long bone and hip fractures. Clinical reviews have evidenced that low BMD and osteoporotic patients show a significant increase in failure of fracture fixation [5, 6]. Moreover, Thormann et al. [7] showed a significant difference in the fracture healing of osteoporotic and healthy animals. Osteoporotic animals showed a significant delay in the bone healing between the stumps of the fracture, with low bone formation and a great amount of connective tissue, even in the long-term follow-up. One of the biggest concerns is the lack of stability, which can lead to pseudarthrosis and infection [5, 6].

The dental implants field brings a well-established concept of coating metal surfaces to improve the bone healing and osseointegration process [8, 9]. It consists of the incorporation of ions naturally present in the bone tissue, such as calcium, phosphorus, and hydroxyapatite. The most commonly used technique is to incorporate these ions through anodization and a biomimetic process [8, 9]. Recently, Marques et al. [10, 11] published two *in vitro* studies presenting a promissing surface coating technique through plasma electrolytic oxidation (PEO), which consists of the incorporation of calcium and phosphorus on the sample surfaces through an electrochemistry reaction with anodic sparks. This process occurs through plasma micro discharges on the surface and has shown superior mechanical and electrochemical properties, besides showing an increase of osteoprogenitor cells around titanium material [10, 11].

Based on such knowledge and taking into consideration that commercially available miniplates do not present a surface coating, a question arose: Could the bioactivity principle by miniplate coating improve bone healing of the fracture gap in BMD situations? Therefore,

this study tested the hypothesis that the use of a bioactive coating (by PEO) on titanium microplates could improve the fracture healing of low BMD rats. Clinically, this could improve the treatment success of osteoporotic patients with bone fractures.

Methods

2 METHODS

Titanium miniplates

Titanium miniplates for internal fixation were supplied from the company (1.5 cm system titanium miniplates with four holes and no intermediate) (Engimplam, Rio Claro, São Paulo, Brazil). Such commercially available miniplates have no surface treatment and were used as a control surface in this study (CONV surface).

Surface coating by plasma electrolytic oxidation (PEO)

The as-received non-coated titanium miniplates were treated using the PEO technique to obtain the experimental surface (PEO surface). The miniplates were treated by means of a pulsed direct current (DC) power supply (Plasma Technology Ltd., Kowloon, Hong Kong, China). The processing system consisted of a stainless-steel tank with a cooling system (cathode) and the miniplates (anode), which were completely submerged in an electrolytic solution that was contained in stainless steel holders. The electrolytic solution was prepared by dissolving 0.3 M of calcium acetate [Ca(C2H3O2)2] (Dinâmica Ltd., Diadema, São Paulo, Brazil) and 0.02 M of glycerophosphate disodium (C3H7Na2O6P) (Sigma-Aldrich, St. Louis, MO, USA) in 500 mL of deionized water. The pH (5.27) and the electrical conductivity (13.8 $mS.cm^{-1}$) of the electrolyte solution were controlled. The pulse voltage, frequency, and duty cycle were established at 290 V, 250 Hz, and 60%, respectively. Deposition was carried out for 10 min, with two miniplates at a time. Then, the treated miniplates were rinsed with deionized water and air dried [12, 13].

Miniplate characterization

The surface topography of the non-coated titanium miniplates and PEO-coated miniplates were analyzed through scanning electron microscopy (SEM) (JEOL JSM-6010LA, Peabody, MA, USA). Energy dispersive spectroscopy (EDS) was used to investigate the chemical composition of the miniplates. The main chemical elements present on each surface were evaluated through a qualitative analysis of the entire spectrum of X-rays in an elementary chemical analysis of 1 μm^3. Three regions of the microplate surface were randomly selected to determine the chemical elements distribution.

In vivo study

Animals and experimental design

This study was approved by the local Ethical Committee on the Use of Animals (FOA no. 00226-2017) and followed the ARRIVE guidelines for animals [14]. A total of 70 six-month-old female rats (*Rattus novergicus albinus* Wistar) weighing approximately 350 g were selected. Animals were kept in cages under temperature control (22 ±2 ºC) and were fed with solid feed (NUVILAB, Curitiba PR, Brazil) and water *ad libitum*. For 10 days, animals were kept without any intervention for acclimatization in the vivarium.

The animals were randomized (www.randomiser.org) regarding their systemic condition (SHAM and OVX groups) and miniplate surface type (CONV and PEO). Four experimental groups were obtained (n = 5): SHAM/CONV included healthy animals that underwent a fake bilateral ovariectomy and received a conventional non-coated surface miniplate on the left femur; SHAM/PEO included healthy animals that underwent a fake surgery and received a PEO-coated miniplate on the right femur; OVX/CONV included animals that underwent a bilateral ovariectomy surgery to induce a condition of osteopenia and received a conventional non-coated surface miniplate on the left femur; and OVX/PEO included animals that underwent a bilateral ovariectomy surgery and received a PEO-coated miniplate on the right femur. Each experimental group was divided into three subgroups (n = 15/group), according to the analysis performed. Additionally, five animals from the OVX and SHAM groups (n = 10) were selected to determine the plasmatic estrogen dosage and bone mechanical properties for osteoporosis validation. The number of animals per group was determined by the power test (Sigma Plot 12.0, San Jose, CA, USA). Data used to perform the power test analysis were extracted from Thormann et al. [15] for a desired power of 90% and alpha of 5%, using the minimal detectable difference in means = 41.11 and expected standard deviation = 13.8; a sample size of 5 per experimental group was expected. (Fig 1).

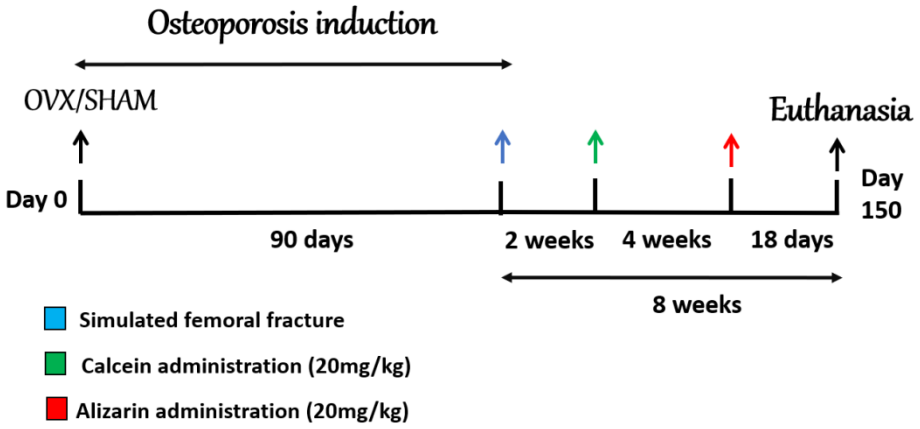


Fig. 1. Experimental design and timeline regarding to osteoporosis induction; fracture simulation and osteosynthesis; administration of fluorochromes of decalcified group and euthanasia.

Bilateral ovariectomy

Animals underwent estrous cycle analysis, in which the vaginal contents were collected to immediately evaluate by electronic microscopy. Only animals presenting a regular cycle were selected for this study. Half of the animals (n = 35) underwent a fake surgery, in which both ovaries were exposed and replaced so that all animals were submitted to the same stress condition (SHAM/CONV and SHAM/PEO). The other animals underwent bilateral ovariectomy to induce the decrease of plasmatic estradiol and the consequent osteopenic condition (OVX/CONV and OVX/PEO). Animals were anesthetized with xylazine (10 mg/kg; p.c., i.m. Coopazine; Coopers Brasil Ltd., Campinas, São Paulo, Brazil) and ketamine hydrochloride injection (50 mg/kg; Vetaset; Fort Dodge Saúde Animal Ltd., Campinas, São Paulo, Brazil), and incisions were made in both flanks, exposing ovaries, followed by their removal. Tissue planes were sutured with Vycril 4-0 (Ethicon, Johnson & Johnson, São José dos Campos, São Paulo, Brazil), and animals received antibiotic injection (0.1 mL/kg; Fort Dodge Saúde Animal Ltd., São Paulo, Brazil) during the immediate postoperative period. After 90 days, five animals from each group (OVX and SHAM) were sacrificed to evaluate the plasmatic estrogen dosage [16, 17] (Fig. 2).

.

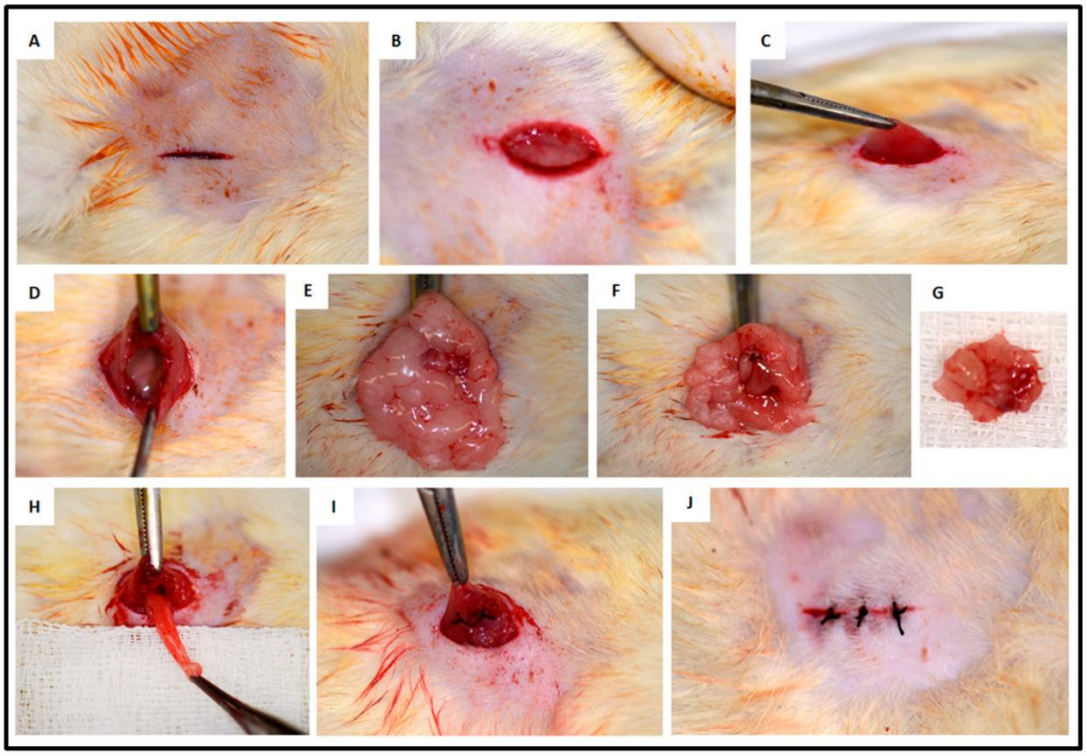


Fig. 2. Stages of the ovariectomy surgical procedure. **(A)** Incision on the flanks of rats; **(B)** Divulsion of the subcutaneous anatomical planes; **(C)** Access to the peritoneum; **(D)** Incision of the peritoneum and access to the abdominal cavity; **(E)** Location of the ovary and uterine horn; **(F)** Tubal ligation of the uterine horn; **(G)** Ovary removed; **(H)** Replacement of lacquered fabrics; **(I)** Suturing the internal planes; **(J)** Suture of the superficial plane.

Estrogen dosage immunoassay

To determine the effectiveness of the ovariectomy, after 90 days of surgery, 5 animals from each group (SHAM and OVX) were sedated. A median laparotomy was performed, and blood samples were collected in heparinized tubes through the inferior vena cava. These samples were centrifuged at 1000 *g* for 15 min at 4 °C, and the plasma obtained was stored at 80 °C until analysis. Estradiol levels were measured using 50 µL of plasma samples for each animal and a monoclonal antibody against rat estradiol (Cat. No. ER1507, ELISA kit for mice Wuhan Fine Biotech Co., Wuhan, China). The absorbance reading was performed at a wavelength of 450 nm in a microplate reader, and the value of the estrogen concentration was expressed in pg/mL.

Biomechanical test for osteoporosis validation

The same animals that received a plasmatic estrogen dosage also had their femurs collected to evaluate the bone mechanical properties and to prove the osteoporosis condition, which was assessed using the three-point bending test (MZ-500S; Maruto Instrument). The tibias were positioned facing upward on a platform, resting on two supports, one anterior and one posterior, with the purpose of stabilizing them and preventing them from moving in any way. A vertical force was applied to the central region of the femurs, at a loading rate of 5 mm/min. Deformation and load curves were used to plot graphs with analysis of the maximum load, stiffness, and breaking energy (energy dissipated by bone before breaking apart) (Fig. 3).

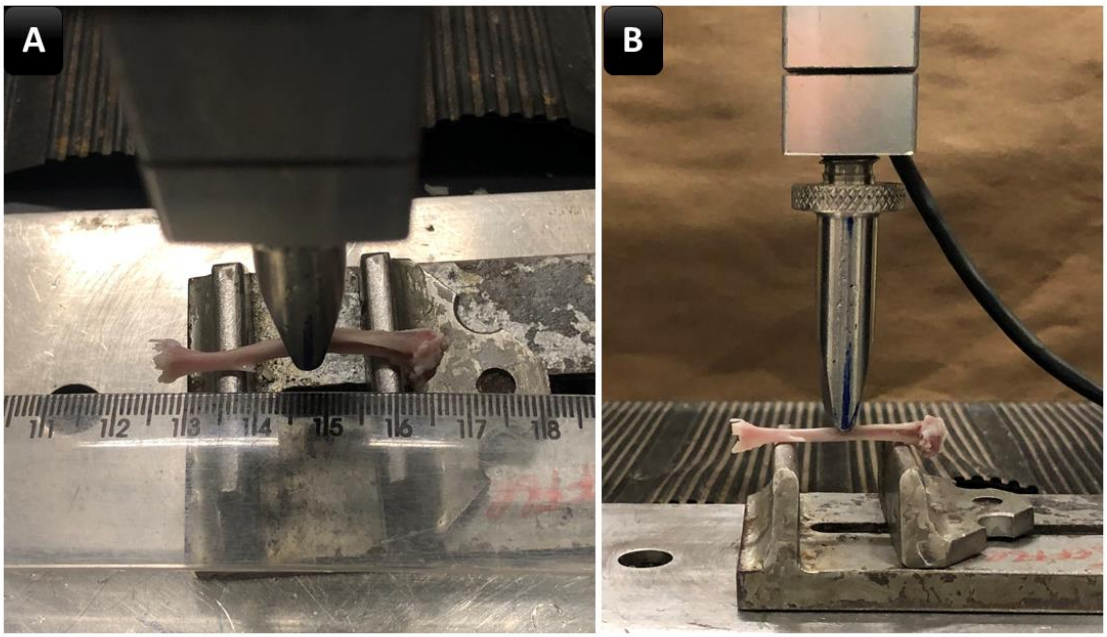


Fig. 3. Biomechanical test for osteoporosis validation. **(A)** Tibia positioned and stabilized by an anterior and posterior support, preventing it to move and **(B)** Application of vertical force in the central region of the femur, at a load rate of 5mm / min.

Femoral fracture simulation

Animals were fasted for 12 h before the bilateral femoral fracture simulation. They were sedated by the combination of intramuscular ketamine (50 mg/kg) (Vetaset – Fort Dodge Saúde Animal Ltd., Campinas, São Paulo, Brazil) and cloridrate of xylazine (5 mg/kg)

(Dopaser – Laboratório Calier do Brasil Ltd., Osasco, São Paulo, Brazil), in addition to a local anesthesia of 0.3 mL/Kg mepivacaine, Scandicaine 2% with adrenaline 1:100.000 (Septodont, Frane) to promote hemostasis. The lateral region of both femurs was trichotomized and antisepsis was conducted with polyvinylpyrrolidone degenerating iodine (PVPI 10%) (Riodeine Degermante, Rioquímica, São José do Rio Preto, Brazil). A 4-cm incision on the lateral femoral region was made to expose the lateral pool of the femoral condyle, between the lateral muscle and the bicep muscle of the femur. A 1.5-mm system titanium miniplate with four holes and no intermediate was fixed bilaterally with 1.5-mm system screws of 4 to 6 mm in length. The non-coated miniplates (CONV) were fixed on the right femur, and the PEO-coated miniplates were fixed on the left femur. Then, the femoral fracture simulation was performed, under saline irrigation, with a circular metal disc through an osteotomy on the epiphyseal metaphysis, between the two most proximal screws, creating a gap of 1 mm [7, 15]. All planes were suturized with resorbable Vycril 4.0 (Ethicon, Johnson Prod., São José dos Campos, São Paulo, Brazil) (Fig. 4). Eight weeks after femoral fracture simulation, animals were euthanized, then subdivided into three groups for analysis: A) analysis of calcified tissues used for microtomography and histometric analysis (n = 5); B) molecular polymerase chain reaction (PCR) analysis (n = 5); and C) biomechanical analysis through biomechanical tests of rigidity and resilience (n = 5).

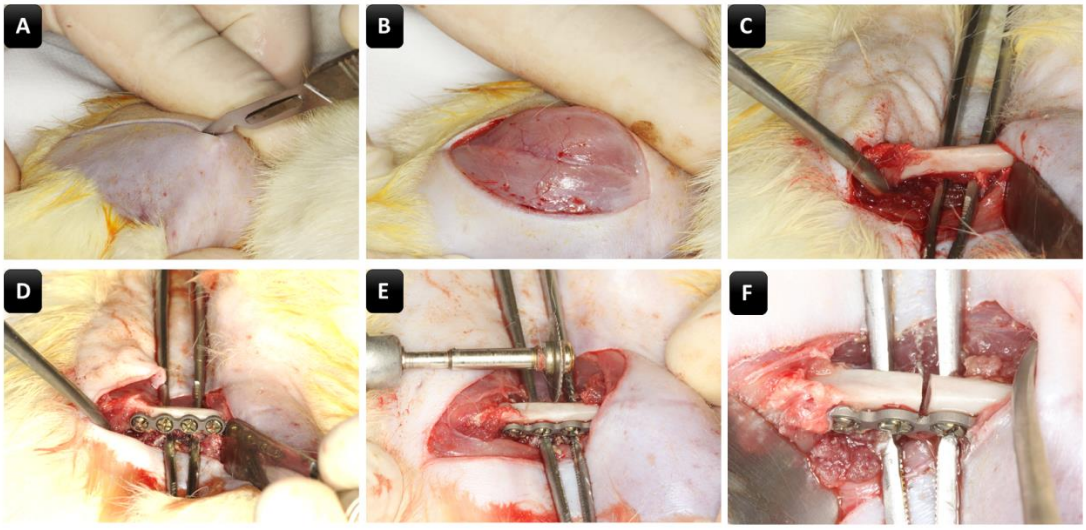


Fig. 4. Stages of the surgical procedure to simulate femoral fractures. **(A)** 4 cm incision in the lateral femoral region; **(B)** Visualization of the lateral muscle and biceps of the femur; **(C)** Exposure of the lateral pole of the femoral condyle; **(D)** Fixing the 1.5 mm titanium miniplate system with four screws and without intermediary; **(E)** 1mm osteotomy in the epiphyseal metaphysis with circular metal disc to simulate femur fracture; **(F)** Final aspect of the osteotomy.

Post-processing analysis

Computed Microtomography

For the three-dimensional structural analysis of bone tissue, the femurs of all groups of animals (n = 5) were removed, reduced, and stored in 70% alcohol, after which they were submitted to X-ray beam analysis in a digital computed microtomography system. The parts were scanned with a SkyScan microtomography device (SkyScan 1176 Bruker MicroCT, Aatselaar, Belgium, 2003) using 8-µm sections (90 Kv and 111 µA) with copper and aluminum filters and a 0.05-mm rotation pitch. Images of the samples obtained by X-ray projection were stored and reconstituted to determine the area of interest using the NRecon software (SkyScan, 2011; Version 1.6.6.0). In the Data Viewer software (SkyScan, Version 1.4.4 64-bit), the images were reconstructed to fit the standard positioning for all samples and were observed in three planes (transverse, longitudinal, and sagittal). Then, using the CTAnalyser (CTAn) software (2003-11 SkyScan, 2012 Bruker MicroCT, Version 1.12.4.0), a 0.25-mm circular area around the osteotomy performed between the two proximal screws (region of interest - ROI) was defined. The CTAn software analyzes and measures images in grayscale (threshold). After adjusting and removing shades of gray, the threshold used in the analysis was 45-255 shades of gray, which allowed us to obtain the volume of bone formed around the gap created (Fig. 5). Therefore, following the volumetric parameters suggested by the American Academy of Mineral Bone Research [18], the parameters related to the amount of bone tissue (BV.TV = percentage of bone volume) and bone tissue quality (Tb.Th = bone trabecular thickness; Tb.Sp = separation of bone trabeculae; and Tb.N = number of trabeculae were obtained.

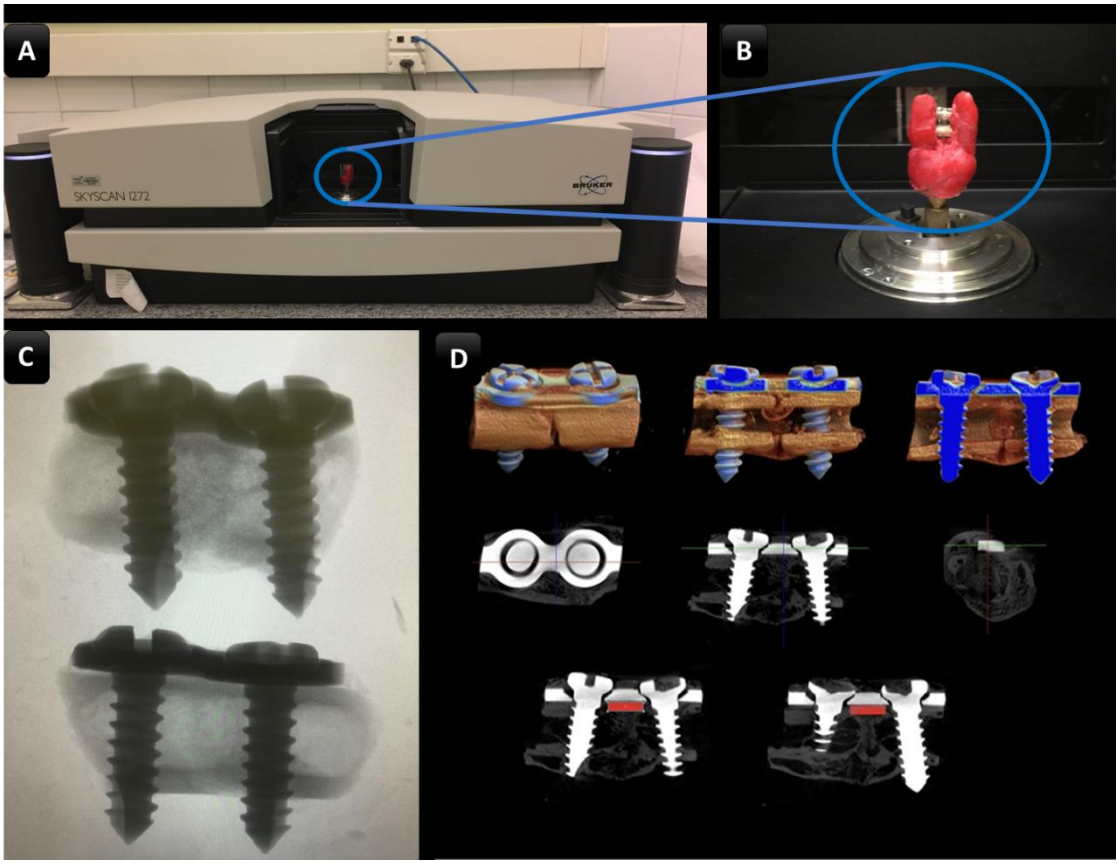


Fig. 5. Procedures for analysis by computed microtomography. **(A)** SkyScan microtomography device; **(B)** Femures positioned and stabilized by acrylic resin on the microtomography device; **(C)** Image obtained by scanning; **(D)** Reconstructions of microtomographic images.

Laser Confocal Microscopy

After the microtomography, bone samples were dehydrated with a gradually increasing sequence of alcohol concentrations (70%, 80%, 90%, 95%, and 100%), and the solution was changed every 3 days. The dehydrated parts were placed in an orbital shaker (KLine CT - 150, Cientec - Laboratory Equipment, Piracicaba, São Paulo, Brazil) every day for 4 h. At the end of the dehydration step, samples were immersed in a mixture of 100% alcohol and embedded in a light-curing TechnoVit® resin (Germany, Heraeus Kulzer GmbH Division Technik Philipp-Reis-Str. 8/13 D-61273 Wehrheim). Then, the embedded femurs were sectioned and worn using an automatic polishing cutting system (Exakt Cutting System, Apparatebau, Gmbh, Hamburg, Germany) until a section approximately 100 µm thick was obtained. The 100-µm thick slides were analyzed in the Leica CTR 4000 CS SPE laser confocal microscope (Leica Microsystems, Heidelberg, Germany) (Fig. 6). The images

obtained from various femoral sections in the region around the gap created between the two most proximal screws were compressed to obtain the best fit. After selecting the thickness, all sections were obtained and operated by means of the z-stack, which allowed us to obtain the best image adjustment to represent the section of each animal in the experimental groups. The images start with the beginning of fluorescence, which in our methodology, represents the beginning of calcification (calcium precipitation in the organic matrix). These images were 1 × 1 mm² in size and corresponded to optical sections of 512 × 512 pixels. Thereafter, 2-µm sections were scanned for 2.5 minutes. Thus, 28 cuts were obtained for each 56-µm scan. The barrier filters used were BP 530/30 nm and 590 LP, combined with the activation of the double dichroic 488/568 nm.

The photomultiplier was adjusted to 534 for calcein and 357 for alizarin. The codes 534 nm and 357 nm represented the filters that facilitated visualization of the fluorochromes. They were located under the microscope, and when light from the mercury lamp passed through these barriers and reached the specimen cuts, it was possible to visualize the fluorochrome colors. The blue filter facilitated the visualization of calcein, and the green filter facilitated the visualization of alizarin. The images obtained via confocal microscopy were reconstituted using confocal microscope manipulation software (Leica CTR 4000 CS SPE, Leica Microsystems, Heidelberg, Germany) [19, 20].

Fluorochromes were applied intramuscularly 2 weeks postoperatively with 20 mg/kg of calcein (green) to represent the old bone and 6 weeks postoperatively with 20 mg/kg of alizarin, a red fluorochrome representing new bone. Bone tissue dynamics are represented by bone turnover, which is observed via red fluorochromes. The higher the prevalence of red fluorescence, the greater the formation of new bone, whereas green fluorescence represents old bone. These dynamics allow us to observe both situations in the same section—in other words, to observe what is new and what is old. The femoral bone (gap area) had two fluorochrome overlays (calcein and alizarin); each overlap represented a calcium precipitation according to each time interval (14 and 42 days), showing the conversion of old bone to new bone. These images were saved in the TIFF format and analyzed using the color threshold tool in Image J (Processing Software and Image Analysis, Ontario, Canada). Each image was standardized according to hue, saturation, and brightness. First, calcein was highlighted, and the “measure” tool was used to provide the area in µm². The same procedure was performed

for alizarin to obtain data on femoral bone dynamics. In this methodological approach, bone turnover was represented by the difference between old bone (green) and new bone (red).

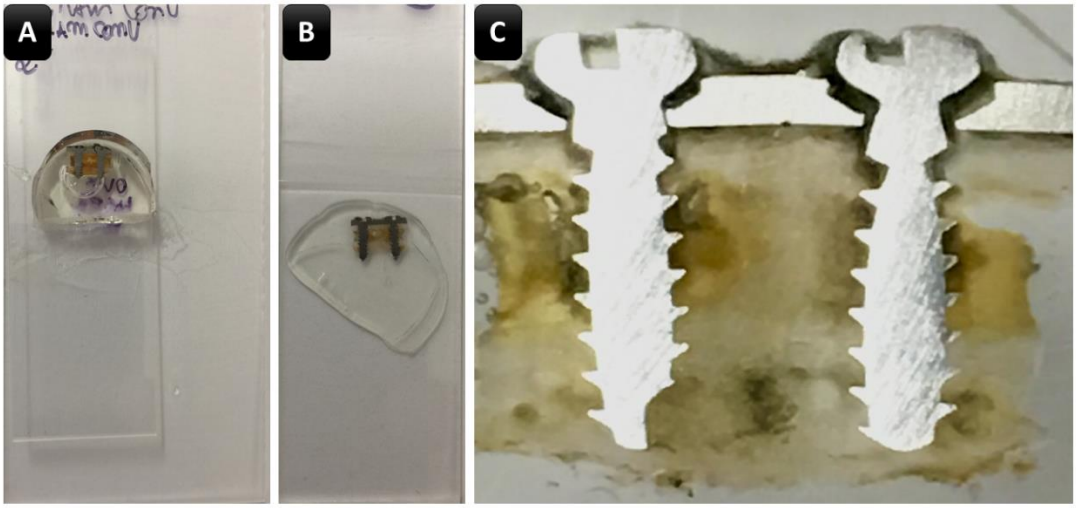


Fig. 6.- (A) Sample of fixed femur after reduction and inclusion on TechnoVit® resin mounted on histological blade. **(B)** Blades obtained after the Exakt cutting until 100 μm thick. **(C)** Region of interest (ROI) between the two most proximal screws and the first third bone/plate complex.

Histometric analysis

After confocal microscopy analysis, samples were washed in deionized water and stained with alizarin red and Stevenel blue. The histological blades were obtained and, after photomicrography of the histological slides, which were saved as TIFF files, the new bone formation (NBF) area was calculated in μm^2 on the most superior third of the gap region, close to the plate, between the two proximal screws, using the Image J software (Processing Software and Image Analysis, Ontario, Canada), through the freehand tool.

Molecular analysis of healing fracture (real-time PCR)

PCR was performed to evaluate the gene expression of markers related to the bone repair process of femoral fracture simulation. PCR plates previously designed by the manufacturer (Applied Biosystems, Foster City, California, USA) were used to enable the expression of genes related to the tissue repair present in exudative, proliferative, and reparative responses until the mineralization of the extracellular matrix of bone tissue

(RUNX-2: runt-related transcription factor 2, BMP2: bone morphogenetic protein 2, COL1: collagen 1, ALP: alkaline phosphatase, OC: osteocalcin, and OSX: osterix). The ROI, the gap fracture healing area, was carefully washed in phosphate buffered saline and frozen in liquid nitrogen so that total RNA could be extracted using Trizol reagent (Life Technologies: Invitrogen, Carslbad, CA, USA). After an analysis of RNA integrity, purity, and concentration, cDNA was created using 1 µg RNA via a reverse transcriptase reaction (M-MLV reverse transcriptase: Promega Corporation, Madison, WI, USA). Sample cDNA was pipetted onto the array PCR plate with Taqman Fast Advanced Mastermix (Applied Biosystems, Foster City, CA, USA) to detect genes involved in the bone repair process (Taqman Array Fast 96 well plate, Applied Biosystems). Real-time PCR was performed on a Step One Plus real-time PCR detection system (Applied Biosystems) under the following conditions: 50 °C (2 min), 95 °C (10 min), 40 cycles of 95 °C (15 s), and 60 °C (1 min), followed by a standard denaturation curve. Relative gene expression was calculated by referencing mitochondrial ribosomal protein expression and normalized by the gene expression of alveolar bone fragments undergoing repair during different experimental periods (ΔΔCT method). The assay was performed in triplicate.

Biomechanical test for bone/miniplates complex

The biomechanical analyses were performed according to Thormann [7]. The bone/miniplate complex was submitted to the three-point test of flexion in a universal testing machine (DL 3000 - EMIC, São José dos Pinhais, Paraná, Brazil) to determine the mechanical properties of the femur submitted to fracture. The extremities of femoral bones were fixed with self-curing acrylic resin to obtain stability during the test. Then, samples were supported on two devices with 55 mm apart between them. A KRATOS® load cell model KM with a capacity of up to 200 kgf was used and connected to a SODEMEX® strain gauge bridge, model CAE201. Deflections were recorded by a Mitutoyo® dial indicator with precision of hundredths of a millimeter. A preload of 0.5 kgf was used to accommodate the system: machine, accessories, and bone, with an accommodation time of 1 min. The speed load was set to 0.50 mm/min. A graph of load versus deflection was obtained and used to calculate the rigidity and resilience of the bone/miniplate system. (Fig 7 A-C).

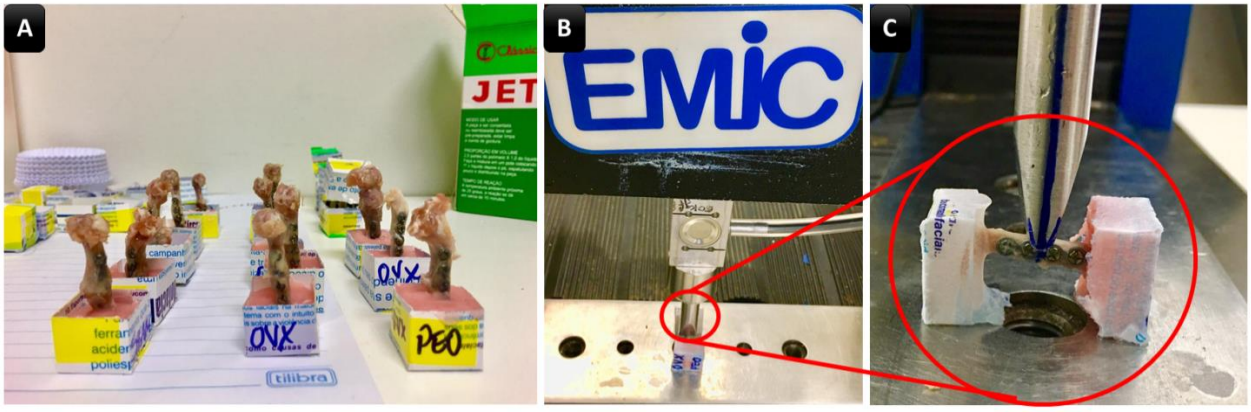


Fig. 7. Procedures for Biomechanical test for bone / miniplates complex. (A) Inclusion of femurs in acrylic resin; **(B)** Femoral stabilized on the DL 3000 universal machine for testing; **(C)** Load cell model used for load application.

Biopsy of metabolizing organs

The same animals used in the biomechanical test had their main organs removed for histopathological analysis. Thus the brain, heart, kidney, liver, lungs, and muscle were collected and immediately fixed in 10% buffered formalin (Merck, Darmstadt, Germany) for 48 h. Samples were microtomized in cuts of 5 μm thickness and stained by hematoxylin and eosin (HE). Histopathological analysis was performed using optical microscopy (Zeiss, Axioshop, Germany), and the characteristics of the organs, such as the presence of cellular or metal infiltrates, hyperplastic tissues, metaplastic or dysplastic transformations, were analyzed among experimental groups [21].

Statistical analysis

The plasmatic estradiol dosage and bone properties (lower breaking force, energy required for fracture and stiffness) were compared between SHAM and OVX groups using the T-test. For quantitative parameters related to PCR, histometric factors, microCT, biomechanical data, and fluorochrome areas (calcein and alizarin red), a two-way ANOVA (factor 1: type of animal, and factor 2: type of miniplate surface) and post Tukey HSD test were used. All tests were performed in the software Sigma-plot 12.0 (Exact graph and data analysis – San José, CA, USA), considering $P < 0.05$ as the level of significance.

Results

3 RESULTS

Surface topography and chemical composition of the miniplates

The photomicrograph of the miniplates coated with PEO showed homogenous surface topography with the presence of pores in a volcano-like geometry while the non-coated miniplate (CONV) showed a smooth surface resulted from the machined process. From the EDS analysis, the elementary chemical composition of the miniplate surface exhibited the presence of titanium and oxygen in both groups, and the successful incorporation of bioactive elements such as calcium (9 wt%) and phosphorus (5 wt%) on the PEO-coated miniplate. The Ca/P ratio (1.8) was similar to the hydroxyapatite (1.67). All elements were homogenously distributed onto the surface which determines the adequate incorporation of the bioactive elements (Fig. 8).

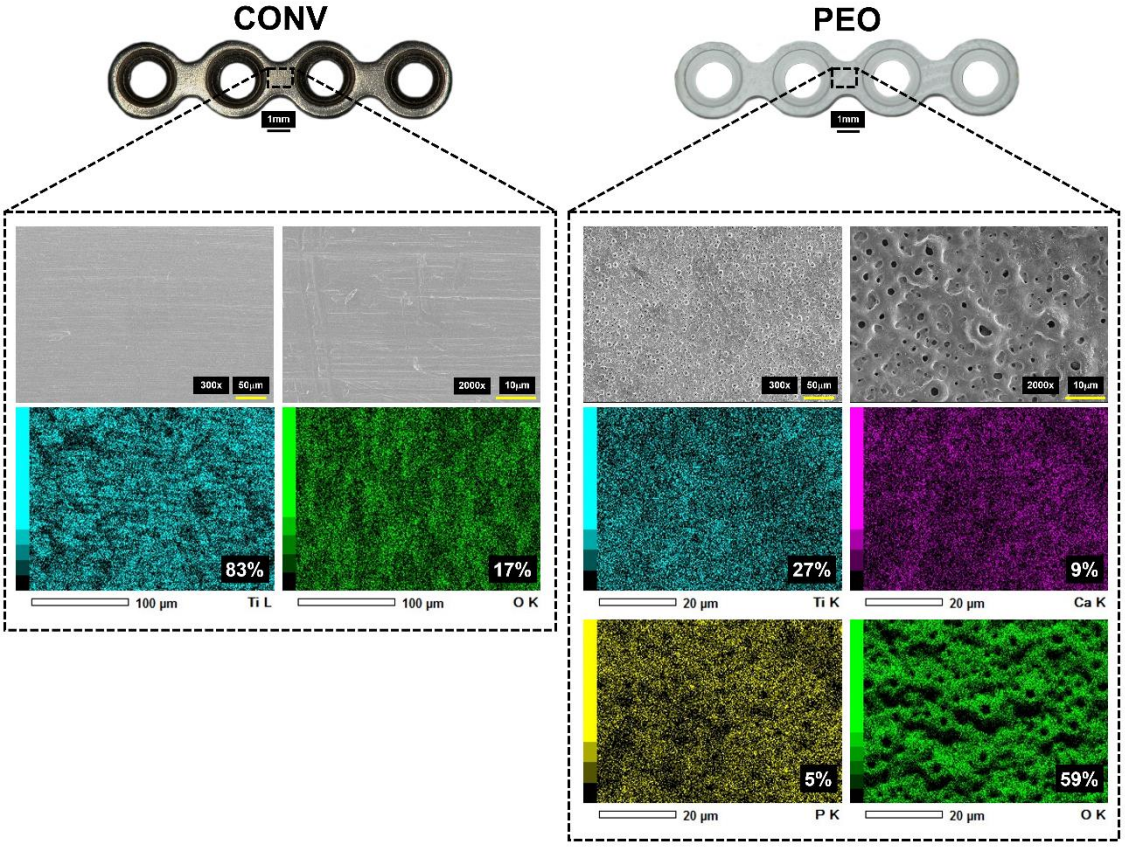


Fig. 8. Images of the as-received non-coated titanium miniplate for internal fixation (CONV) and PEO-coated titanium miniplate (top images). Representative micrographs of scanning electron microscopy in the magnitudes of 300× and 2000× of CONV and PEO-coated miniplates (middle images). Color figures show the chemical mapping of microplate surfaces by EDS with element concentration (wt%) (Ti, O, Ca and P).

Osteoporosis condition validation

The plasmatic estradiol dosage showed a significant decrease of plasmatic estradiol 3 months after the animals underwent a bilateral ovariectomy (OVX: 8.33 ±2.18 pg/mL) compared to animals that underwent a fake surgery (SHAM: 58.19 ±19.00 pg/mL) ($P < 0.001$; T-test), showing the effectiveness of the ovariectomy. The bone biomechanical test showed lower breaking force ($P = 0.018$), energy required for fracture ($P = 0.022$), and stiffness ($P = 0.002$) for the OVX group compared to the SHAM group (Table 1). The reduced bone mechanical properties and the low estrogen level indicated the osteoporosis condition in the OVX group.

Table 1

Mechanical data of femur bone from OVX and SHAM groups. Data are expressed as mean ±standard deviation.

Group	Breaking force (N)	Rigidity (KN/m)	Energy (mJ)
OVX	47.01 ±11.39 [a]	75.57 ±12.26 [a]	16.38 ±7.15 [a]
SHAM	67.35 ±7.29 [b]	117.88 ±15.37 [b]	25.63 ±3.24 [b]

Means followed by different lowercase letter in column differ ($P < 0.05$) by T-test.

Fluorochrome area

The representative photomicrographs of calcein and alizarin precipitation and the quantitative fluorochrome areas showed a greater precipitation of calcein (green area) than alizarin (red area) in both OVX groups, indicating higher amounts of old bone. However, the PEO surface showed a lower amount of both fluorochromes than the CONV surface for the OVX and SHAM groups with statistically significant reduction in the calcein content ($P < 0.05$) (Fig. 9 and 10).

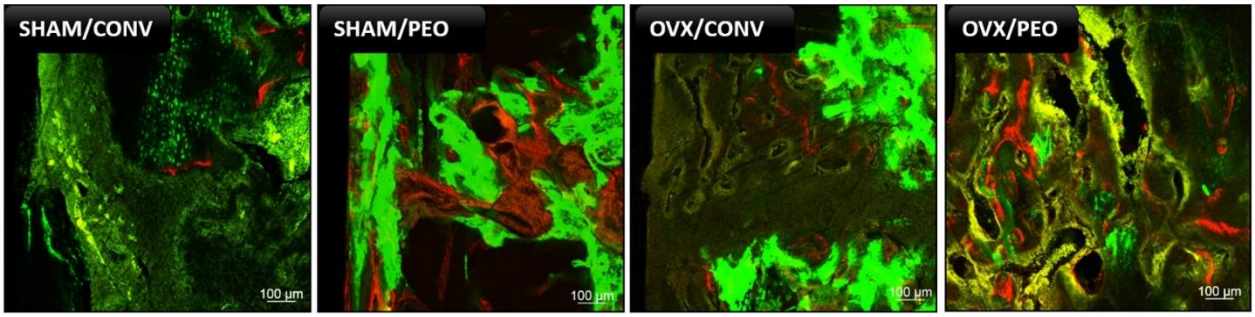


Fig. 9. Laser confocal microscopy photomicrographs of the slides (10× magnification) (bottom figures). The green color represents fluorochrome calcein (old bone), and the red color represents precipitation of alizarin (new bone). Bar = 100 µm.

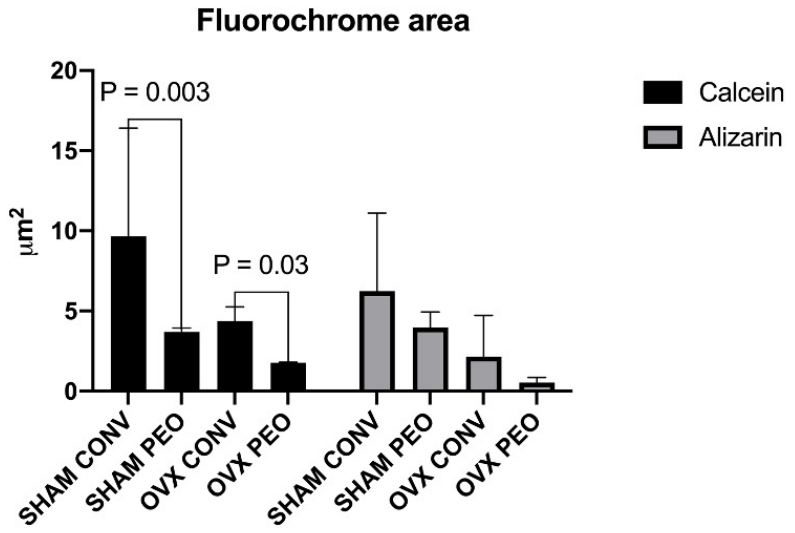
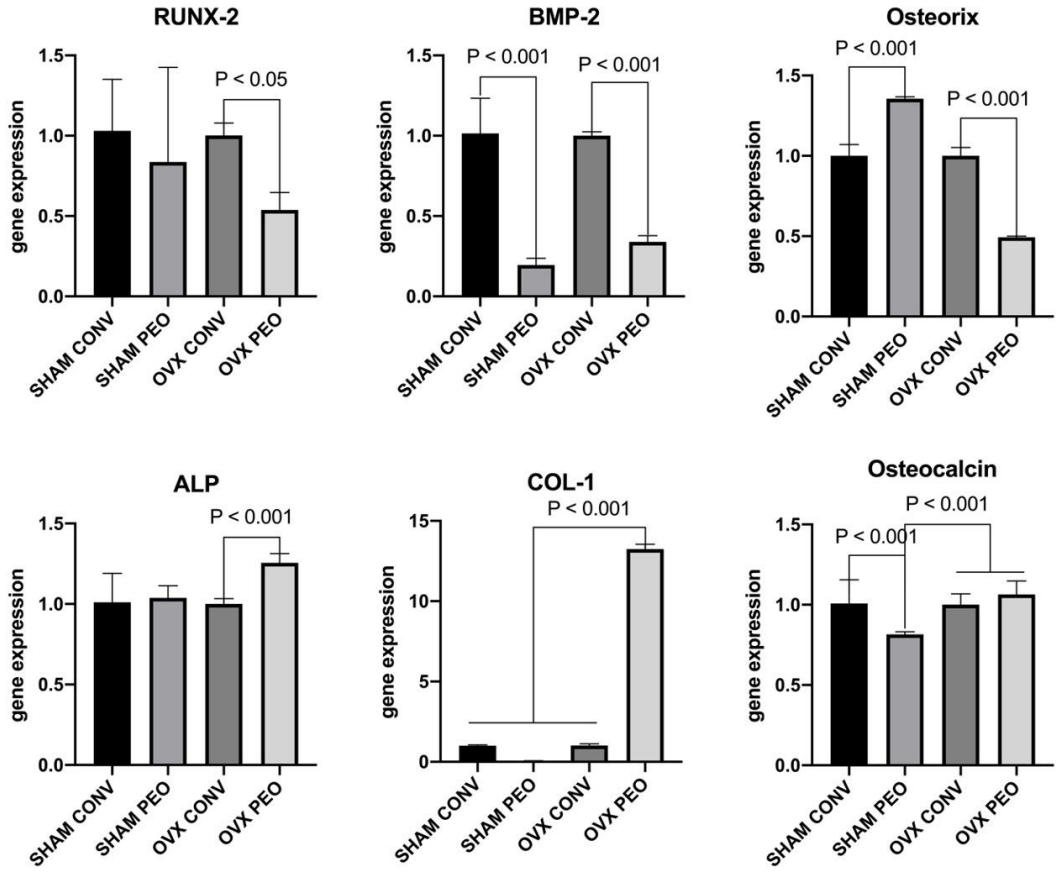


Fig. 10. Quantitative area (in µm^2) of calcein and alizarin fluorochromes (top image). The statistical difference between groups is showed with the p-value in the figure. Data are expressed as mean ± standard deviation.

Molecular analysis of healing fracture (real-time PCR)

Regarding the gene expression results by real-time PCR, the OVX/PEO group showed significantly lower values for RUNX-2 (OVX/CONV: 1.00 ±0.07; OVX/PEO: 0.53 ±0.10), BMP-2 (OVX/CONV: 1.00 ±0.02; OVX/PEO: 0.33 ±0.03), and osterix (OVX/CONV: 1.00 ±0.05; OVX/PEO: 0.49 ±0.01) compared to the OVX/CONV group ($P < 0.05$). Regarding the osteoblastic protein ALP, the OVX/PEO (1.25 ±0.05) group showed significantly higher values compared to the OVX/CONV (1.00 ±0.03) group ($P < 0.05$). Regarding the

mineralization protein COL1, significantly higher values were found for the OVX/PEO (13.23 ±1.75) group compared to the other groups ($P < 0.001$). Furthermore, the PEO (1.06 ±0.08) surface showed a tendency toward higher values for compared to CONV (1.00 ±0.06) for the OVX groups (Fig. 11).



OCN

Fig. 11. Gene expression by real-time PCR of RUNX-2 (runt-related transcription factor 2), BMP-2 (bone morphogenetic protein 2), Osterix, ALP (alkaline phosphatase), COL-1 (collagen 1) and Osteocalcin. The statistical difference between groups is showed with the p-value in the figure. Data are expressed as mean ± standard deviation.

Histometric analysis

The qualitative histological results showed that ovariectomized animals (OVX groups) exhibited poorer bone formation during femoral fracture healing than the SHAM groups. However, the PEO surface showed greater presence of bone tissue in all extensions on the gap of the fracture compared to the CONV surface, which showed greater presence of connective and adipose tissue, mainly on the second third of the gap fracture. The histological

characteristics of the OVX/PEO group resembled those of the SHAM/CONV group (Fig. 12). The quantitative histometric results regarding the new bone formation showed that PEO was able to increase the new bone formation in the SHAM (P = 0.003) and OVX (P = 0.004) groups. It is interesting to note that the OVX/PEO exhibited similar values when compared with those of SHAM/CONV group (Fig. 13).

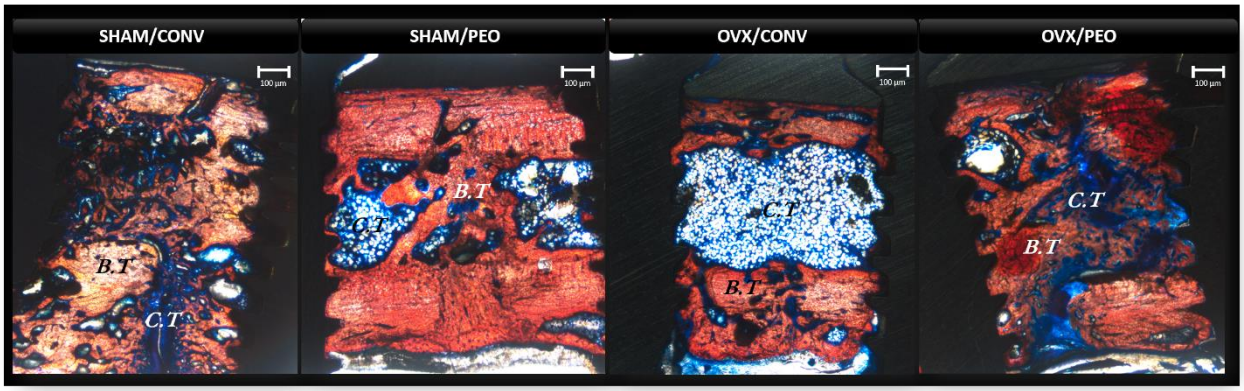


Fig. 12. Photomicrographs of histological slides stained with Stevenel blue and alizarin red (25× magnification), showing a great aspect of new bone formation during femoral healing of OVX/PEO and little presence of adipose and connective tissue. The OVX/CONV group showed few areas of new bone formation and significant presence of adipose and connective tissue. BT – bone tissue; CT – connective tissue. Bar = 100 µm.

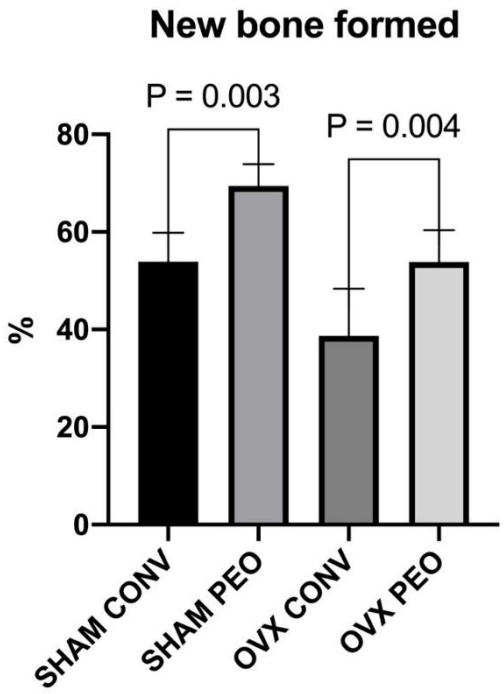


Fig. 13. New bone formation (in %) evaluated by histometric analysis. The statistical difference between groups is showed with the p-value in the figure. Data are expressed as mean ± standard deviation.

Computed microtomography

The bone formation parameters obtained through computed microtomography showed that the BV.TV values tended to be higher for the SHAM groups compared with the OVX groups ($P < 0.05$). However, no significant difference was noted between the surfaces of the microplates ($P > 0.05$). Tb.Th data were similar among groups ($P > 0.05$). For qualitative parameters such as Tb.N significantly higher values were found for the OVX/PEO group compared to the OVX/CONV group ($P < 0.05$). In the Tb.Sp analysis, PEO group exhibited greater values than the CONV surface for both SHAM and OVX conditions ($P < 0.05$) (Fig. 14)

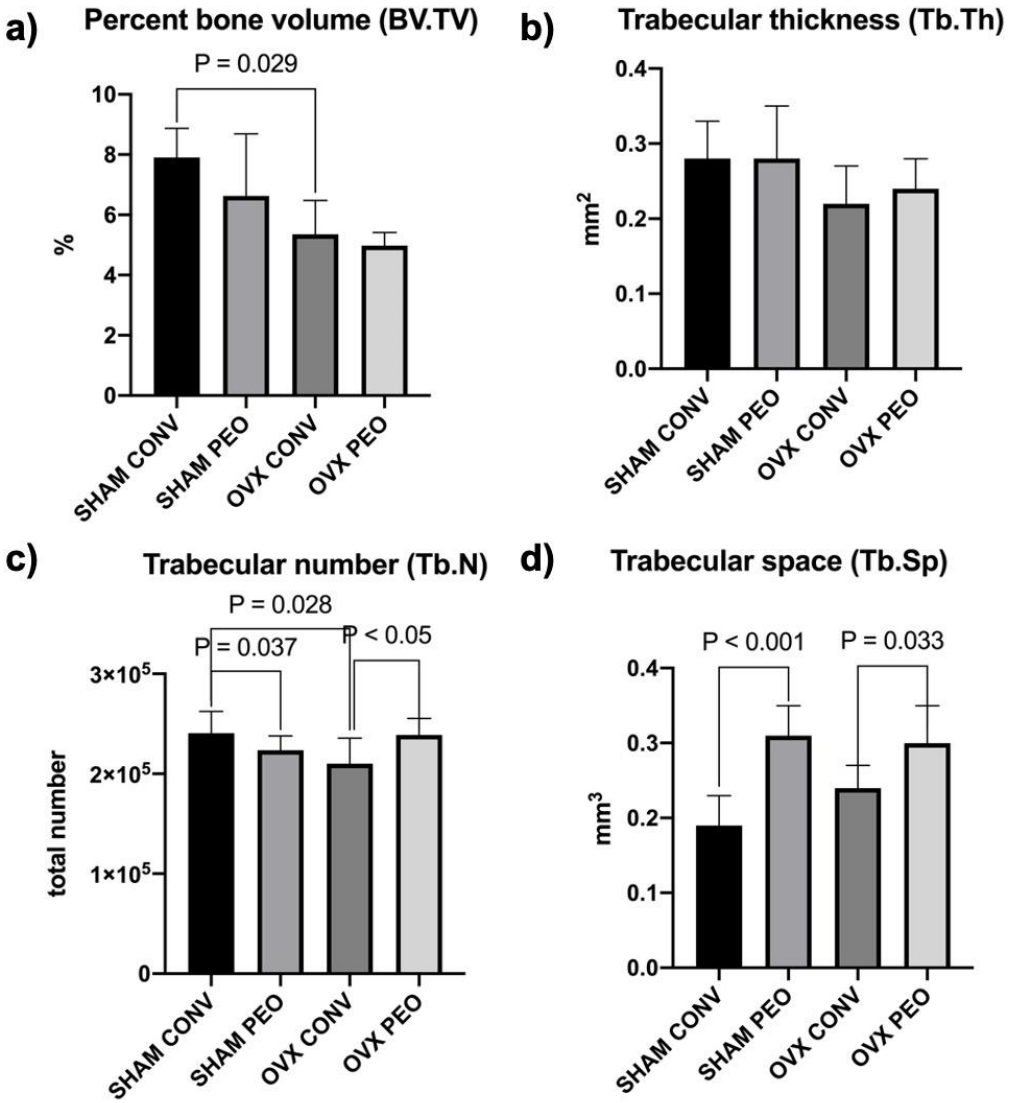


Fig. 14. Bone formation parameters obtained through computed microtomography. **(a)** Percent bone volume (BV.TV) (unit: %) **(b)** Trabecular thickness (Tb.Th) (unit: mm^2). **(c)** Trabecular number (Tb.N) (unit: total number). **(d)** Trabecular space (Tb.Sp) (unit: mm^3). The statistical difference between groups is showed with the p-value in the figure. Data are expressed as mean ± standard deviation.

Biomechanical test

The resilience values of the bone/microplate system obtained through a biomechanical test were the greatest in the OVX/PEO group compared to the other groups ($P < 0.05$) (Fig. 15).

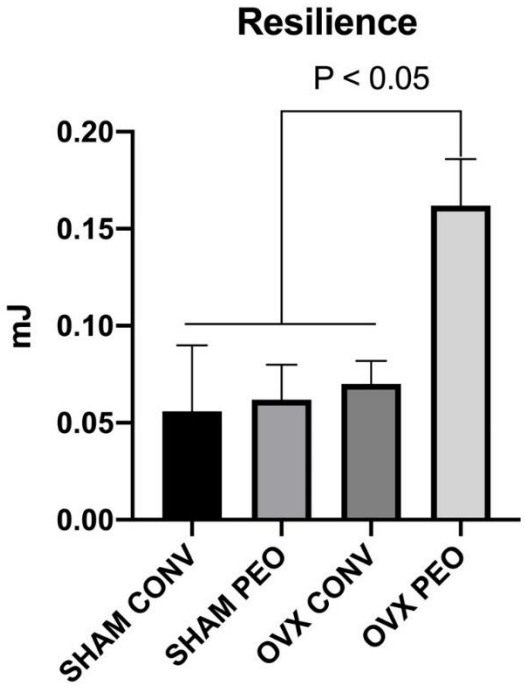


Fig. 15. Bone resilience (in mJ) values obtained in the biomechanical test by 3 points flexion. The statistical difference between groups is showed with the p-value in the figure. Data are expressed as mean ± standard deviation.

Biopsy of metabolizing organs

The metabolizing organs (brain, heart, kidney, liver, lungs, and muscle) showed no structural changes for both types of miniplate surface (Fig. 8). Under the light microscopy, the liver presented hepatocytes with normal characteristics, structurally organized in hepatic lobes, with all its constituent elements present (blood vessels and bile ducts). The kidney presented well-organized and delimited renal corpuscles, interspersed with the system of tubules and ducts that are specific to this tissue. Regarding the muscle tissue, the skeletal striated muscle exhibited its conventional histological aspects, with elongated cells; peripherally multinucleated, transverse striations; scarcity of extracellular matrix between

them; and organization in fascicles covered by normal-looking connective tissue. The striated cardiac muscle, observed in the myocardial region (heart), presented cells with characteristic striations and centralized nuclei, joined by means of intercalated discs. The brain showed a highly cellularized cortical region, with evident neuronal bodies and neuroglia, and a white substance rich in nerve fibers and cellular extensions. The pulmonary parenchyma of the alveolar region showed structurally organized saccular structures, with typical cells and abundant blood vessels. (Fig. 16).

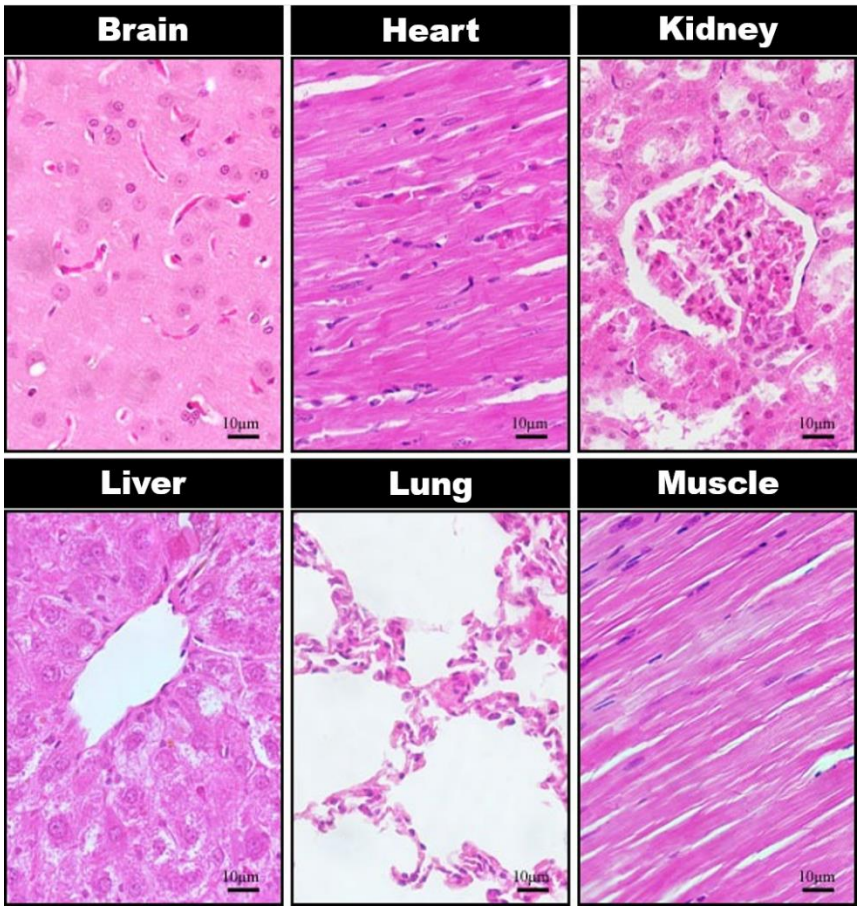


Fig. 16. Photomicrographs (40× magnification) from organs (brain, heart, kidney, liver, lungs, and skeletal striated muscle) to observe the presence of possible contamination by metal ions from the microplates. Bar = 10 µm.

Discussion

4 DISCUSSION

This animal study aimed to evaluate the biological, structural, and mechanical behavior during femoral fracture healing simulation in animals with low BMD fixed by titanium miniplates coated using the PEO technique. Animals with low BMD, which received miniplates coated by PEO (OVX/PEO), showed structural parameters compatible with osteoporotic characteristics. However, they also showed an increase in bioactivity of the osteoprogenitor cells and a significant bone formation in the gap of the fracture. Furthermore, the low BMD animals that received PEO-coated miniplates showed a significant increase in resilience of the bone/microplate system compared to other groups.

Despite no clinical consensus about the fracture healing in low BMD circumstances being significantly delayed compared to in healthy bone [22], some experimental studies showed a significant difference around 6 weeks of a 3-mm femoral fracture healing in the comparison between ovariectomized and healthy animals [7]. Additionally, a clinical study showed a predicted major reoperation for 120 low BMD and alcoholic patients younger than 70 years old with femoral and neck fractures [6]. For this reason, the current study adopted the low BMD animal model, inducing an osteoporosis condition in the animals through bilateral ovariectomy and 3 months of expectation. There was a significant difference in the plasmatic estrogen dosage between the OVX and SHAM groups, compatible with osteopenic condition, according to Food and Drug Administration (FDA) [23]. Furthermore, the osteoporosis condition was proved by the results obtained through biomechanical tests, which showed a great difference in resistance to fracture between tibias when comparing OVX to SHAM groups, validating this experimental model.

To establish the problematic condition of fracture healing in low BMD conditions, an unedited animal model of fracture healing with surface-coated titanium miniplates was employed, and the technique of surface coating by PEO has shown promising results in *in vitro* studies with titanium discs [10, 11] and *in vivo* studies with dental implants [24]. These authors showed that PEO-coated surfaces increased osteoblastic activity and NBF during peri-implant healing, as well as presenting greater hardness and resistance to corrosion. The current study showed that PEO was effective to incorporate calcium and phosphorous on the miniplate surface. Furthermore, SEM showed a homogeneous distribution of pores on the microplate surface, a property that provides an improvement in cellular adhesion and consequently greater bone formation during fracture healing.

Structural parameters collected by computed microtomography showed that osteoporotic animals had lower bone volume and trabecular thickness than healthy animals. Additionally, PEO coating does not improve these features. Furthermore, there was a greater trabecular number and trabecular space in the low BMD animals (OVX) that received PEO-coated microplates than in the non-coated CONV microplate animals, characterizing low bone quality. It is important to clarify that these results were expected because our animals with BMD did not receive any systemic drug treatment for osteoporosis condition. Therefore, no exceptional improvement of bone microarchitecture during 8 weeks of fracture healing was expected because of the microplate surface coating.

The microarchitecture pattern corroborates with the bone dynamics findings, which showed a higher amount of green calcein than alizarin red deposited on bone tissue for both OVX groups. These data indicate a greater presence of old bone compared to new bone formed in low BMD animals, which was also expected. However, it is necessary to highlight that the OVX/PEO group showed a lower amount of both fluorochromes' precipitation than the OVX/CONV group, as well as a minimal difference between calcein and alizarin, denoting a great balance in bone remodeling. These findings suggest that the PEO surface provides an anticipation of bone formation in low BMD animals, before the administration of fluorochromes, during 8 weeks of fracture healing.

This statement seems to be reasonable, because data from PCR molecular analysis showed that after 8 weeks of fracture healing, the expression of pre-osteoblastogenic proteins RUNX-2, BMP-2, and osterix were significantly lower in low BMD animals that received PEO-coated microplates than in those that received non-coated CONV microplates. Nevertheless, the expression of proteins related to the middle and final phases of bone formation, such as ALP and COL-1, were significantly superior in the OVX/PEO group than in the OVX/CONV group. These results support the hypothesis of anticipation of bone formation in low BMD conditions with PEO surface microplates. Indeed, studies have shown that pre-osteoblastogenic proteins are expressed during earlier periods, such as after 1 and 2 weeks of bone remodeling, whereas the osteoblastic and mineralized proteins are expressed after 4 weeks of bone remodeling [25-27]. These data prove that low BMD animals with CONV surface microplates showed a delay in fracture healing and confirm the earlier bone formation in the OVX/PEO group.

Moreover, the enhancement of NBF in low BMD animals with PEO surface microplates can also be observed through histometric analysis. The OVX/PEO group showed greater bone formation than the OVX/CONV group, which showed a significant presence of adipose and connective tissue. Besides greater NBF, the PEO-coated microplate/femoral bone system showed a significantly higher resilience during mechanical tests than the non-coated CONV microplates in low BMD animals. This high discrepancy in mechanical tests for PEO surface microplates seems to be related to the increased expression of the COL1 protein [28]. Furthermore, a study by Beline et al. [29] showed that texturing by PEO increased the mechanical resistance of titanium material.

Another important point to discuss is the fact that all organs showed no structural changes in both microplate surface conditions. These data might suggest an anti-corrosive/tribocorrosive effect of PEO, probably due the great electrochemical stability provided by this type of coating [30]. It has been a significant challenge in the biomedical field to develop a type of alloy in materials for internal fixation that presents a corrosion-resistance property. Jacobs et al. [31] reported that metal from orthopedic implants underwent a significant effect of corrosion, and the ions released could be found in the tissue around the material, as well as on metabolizing organs. Herein, the absence of metal ions in the metabolizing organs could be attributed to the short term of bone fixation compared to the clinical situation, where the microplates are removed after many years or remain for the patient's entire life [32, 33]. Even so, these findings are encouraging and provide new perspectives on PEO-coated microplates applications.

Indeed, this study presents limitations, because this is a preclinical model in rats. Earlier periods of femoral fracture healing could be evaluated to obtain deep molecular analysis. Furthermore, 8 weeks of fracture healing is a short time when compared to the long-term clinical follow-up. Our animals were not treated to reduce the osteoporosis condition, and normally patients receive medical treatment for this condition when undergoing internal fixation, which generates some bias in the current study. Thus, the authors encourage other studies to obtain more evidence on this issue.

The treatment of orthopedic and maxillofacial fractures in patients with low BMD is a significant challenge. There are several cases in which there is no explanation for the non-union fracture healing, which leads to severe sequels for patients. This preclinical model showed encouraging results for PEO-coated miniplates for internal fixation on simulated

femoral fractures. PEO coating produced improved cellular activity, stimulating pre-osteogenic cells earlier than non-treated microplate surfaces in low BMD animals. Furthermore, there was greater NBF for the PEO-coated microplate surface, very similar to the bone formed from the non-coated microplate surface of healthy animals, which is the gold standard for most surgical treatments employed.

References

REFERENCES

[1] A. Liedert, D. Kaspar, P. Augat, A. Ignatius, L. Claes, Mechanobiology of bone tissue and bone cells, in: A. Kamkin, I. Kiseleva (Eds.), Mechanosensitivity in cells and tissues, Academia, Moscow, 2005.

[2] E. Gomez-Barrena, P. Rosset, D. Lozano, J. Stanovici, C. Ermthaller, F. Gerbhard, Bone fracture healing: cell therapy in delayed unions and nonunions, Bone 70 (2015) 93-101.

[3] L. Claes, S. Recknagel, A. Ignatius, Fracture healing under healthy and inflammatory conditions, Nat Rev Rheumatol 8 (2012) 133-143.

[4] M.L. Fernandez Soto, A. Gonzalez Jimenez, M. Varsavsky, Bone metabolism and fracture risk in anorexia nervosa, Med Clin 135 (2010) 274-279.

[5] C. von Ruden, P. Augat, Failure of fracture fixation in osteoporotic bone, Injury 47 (2016) S3-S10.

[6] P. Campenfeldt, A. Al-Ani, M. Hedstrom, W. Ekstrom, Low BMD and high alcohol consumption predict a major re-operation in patients younger than 70 years of age with a displaced femoral neck fracture-A two -year follow up study in 120 patients, Injury 49 (2018) 2042-2046.

[7] U. Thormann, T. El Khawassna, S. Ray, L. Duerselen, M. Kampschulte, K. Lips, H. von Dewitz, S. Heinemann, C. Heiss, G. Szalay, A.C. Langheinrich, A. Ignatius, R. Schnettler, V. Alt, Differences of bone healing in metaphyseal defect fractures between osteoporotic and physiological bone in rats, Injury 45 (2014) 487-493.

[8] T.P. Queiroz, F.A. Souza, A.C. Guastaldi, R. Margonar, I.R. Garcia-Junior, E. Hochuli-Vieira, Commercially pure titanium implants with surfaces modified by laser beam with and without chemical deposition of apatite. Biomechanical and topographical analysis in rabbits, Clin Oral Implants Res 24 (2013) 896-903.

[9] W. Luo, J. Zhao, X. Meng, S. Ma, Q. Sun, T. Guo, Y. Wang, Y. Zhou, Effect of zinc doped calcium phosphate coating on bone formation and the underlying biological mechanism, Sheng Wu Yi Xue Gong Cheng Xue Za Zhi 32 (2015) 1359-1363.

[10] I.D. Marques, V.A. Barao, N.C. da Cruz, J.C. Yuan, M.F. Mesquita, A.P. Ricomini-Filho, C. Sukotjo, M.T. Mathew, Electrochemical behavior of bioactive coatings on cp-Ti surface for dental application, Corros Sci 100 (2015) 133-146.

[11] I.S.V. Marques, N.C. Cruz, R. Landers, J.C. Yuan, M.F. Mesquita, C. Sukotjo, M.T. Mathew, V.A. Barao, Incorporation of Ca, P, and Si on bioactive coatings produced by plasma electrolytic oxidation: The role of electrolyte concentration and treatment duration, Biointerphases 10 (2015) 041002.

[12] I.S.V.Marques, V.A.R. Barão, N.C. Cruz, J.C.C. Yuan, M.F. Mesquita, A.P. Ricomini Filho, C. Sukotjo, M.T. Mathewe, Electrochemical behavior of bioactive coatings on cp-Ti surface for dental application, Corrosion Science 100 (2015) 133-146.

[13] I.S.V. Marques, N.C. Cruz, R. Landers, J.C.C. Yuan, M.F. Mesquita, C. Sukotjo, M.T. Mathew, V.A.R. Barão, Incorporation of Ca, P, and Si on bioactive coatings produced by plasma electrolytic oxidation: the role of electrolyte concentration and treatment duration, Biointerphases 10 (2015) 1-11.

[14] C. Kilkenny, W. Browne, I.C. Cuthill, M. Emerson, D.G. Altman, N.C.R.R.G.W. Group, Animal research: reporting in vivo experiments: the ARRIVE guidelines, Br J Pharmacol 160 (2010) 1577-1579.

[15] U. Thormann, S. Ray, U. Sommer, T. Elkhassawna, T. Rehling, M. Hundgeburth, A. Henss, M. Rohnke, J. Janek, K.S. Lips, C. Heiss, G. Schlewitz, G. Szalay, M. Schumacher, M. Gelinsky, R. Schnettler, V. Alt, Bone formation induced by strontium modified calcium phosphate cement in critical-size metaphyseal fracture defects in ovariectomized rats, Biomaterials 34 (2013) 8589-8598.

[16] E.R. Luvizuto, S.M. Dias, T.P. Queiroz, T. Okamoto, I.R. Garcia, Jr., R. Okamoto, R.C. Dornelles, Osteocalcin immunolabeling during the alveolar healing process in ovariectomized rats treated with estrogen or raloxifene, Bone 46 (2010) 1021-1029.

[17] G. Ramalho-Ferreira, L.P. Faverani, G.A.C. Momesso, E.R. Luvizuto, I. de Oliveira Puttini, R. Okamoto, Effect of antiresorptive drugs in the alveolar bone healing. A histometric and immunohistochemical study in ovariectomized rats, Clin Oral Investig 21 (2017) 1485-1494.

[18] M.L. Bouxsein, S.K. Boyd, B.A. Christiansen, R.E. Guldberg, K.J. Jepsen, R. Muller, Guidelines for assessment of bone microstructure in rodents using micro-computed tomography, J Bone Miner Res 25 (2010) 1468-1486.

[19] V. Papalexiou, A.B. Novaes, Jr., M.F. Grisi, S.S. Souza, M. Taba, Jr., J.K. Kajiwara, Influence of implant microstructure on the dynamics of bone healing around immediate implants placed into periodontally infected sites. A confocal laser scanning microscopic study, Clin Oral Implants Res 15 (2004) 44-53.

[20] G. Ramalho-Ferreira, L.P. Faverani, G.A. Grossi-Oliveira, T. Okamoto, R. Okamoto, Alveolar bone dynamics in osteoporotic rats treated with raloxifene or alendronate: confocal microscopy analysis, J Biomed Opt 20 (2015) 038003.

[21] R. Piozzi, D.A. Ribeiro, L.E. Padovan, H. Nary Filho, M.A. Matsumoto, Genotoxicity and cytotoxicity in multiple organs induced by titanium miniplates in Wistar rats, J Biomed Mater Res A 88 (2009) 342-347.

[22] N. Mathavan, M.J. Turunen, M. Guizar-Sicairos, M. Bech, F. Schaff, M. Tagil, H. Isaksson, The compositional and nano-structural basis of fracture healing in healthy and osteoporotic bone, Sci Rep 8 (2018) 1591.

[23] D.D. Thompson, H.A. Simmons, C.M. Pirie, H.Z. Ke, FDA Guidelines and animal models for osteoporosis, Bone 17 (1995) 125S-133S.

[24] G.A.C. Momesso, A.M. de Souza Santos, E.S.J.M. Fonseca, N.C. da Cruz, R. Okamoto, V.A.R. Barao, R.S. Siroma, J.A. Shibli, L. Perez Faverani, Comparison between plasma electrolytic oxidation coating and sandblasted acid-etched surface treatment: histometric, tomographic, and expression levels of osteoclastogenic factors in osteoporotic rats, Materials 13 (2020) 1604.

[25] F.C. Yogui, G.A.C. Momesso, L.P. Faverani, T.O.B. Polo, G. Ramalho-Ferreira, J.S. Hassumi, A.C. Rossi, A.R. Freire, F.B. Prado, R. Okamoto, A SERM increasing the expression of the osteoblastogenesis and mineralization-related proteins and improving quality of bone tissue in an experimental model of osteoporosis, J Appl Oral Sci 26 (2018) e20170329.

[26] J.S. Hassumi, G. Mulinari-Santos, A. Fabris, R.G.M. Jacob, A. Goncalves, A.C. Rossi, A.R. Freire, L.P. Faverani, R. Okamoto, Alveolar bone healing in rats: micro-CT, immunohistochemical and molecular analysis, J Appl Oral Sci 26 (2018) e20170326.

[27] Y.X. He, G. Zhang, X.H. Pan, Z. Liu, L.Z. Zheng, C.W. Chan, K.M. Lee, Y.P. Cao, G. Li, L. Wei, L.K. Hung, K.S. Leung, L. Qin, Impaired bone healing pattern in mice with ovariectomy-induced osteoporosis: a drill-hole defect model, Bone 48 (2011) 1388-400.

[28] H.L. Gooch, J.E. Hale, H. Fujioka, G. Balian, S.R. Hurwitz, Alterations of cartilage and collagen expression during fracture healing in experimental diabetes, Connect Tissue Res 41 (2000) 81-91.

[29] T. Beline, S. Marques Ida, A.O. Matos, E.S. Ogawa, A.P. Ricomini-Filho, E.C. Rangel, N.C. da Cruz, C. Sukotjo, M.T. Mathew, R. Landers, R.L. Consani, M.F. Mesquita, V.A. Barao, Production of a biofunctional titanium surface using plasma electrolytic oxidation and glow-discharge plasma for biomedical applications, Biointerphases 11 (2016) 011013.

[30] I. Marques, M.F. Alfaro, N.C.D. Cruz, M.F. Mesquita, C. Takoudis, C. Sukotjo, M.T. Mathew, V.A.R. Barao, Tribocorrosion behavior of biofunctional titanium oxide films produced by micro-arc oxidation: Synergism and mechanisms, J Mech Behav Biomed Mater 60 (2016) 8-21.

[31] J.J. Jacobs, J.L. Gilbert, R.M. Urban, Corrosion of metal orthopaedic implants, J Bone Joint Surg Am 80 (1998) 268-282.

[32] S.G. Steinemann, Metal implants and surface reactions, Injury 27 (1996) SC16-SC22.

[33] R.M. Urban, J.J. Jacobs, M.J. Tomlinson, J. Gavrilovic, J. Black, M. Peoc'h, Dissemination of wear particles to the liver, spleen, and abdominal lymph nodes of patients with hip or knee replacement, J Bone Joint Surg Am 82 (2000) 457-476.

Anexos

ANEXO A – Certificado do Comitê de Ética

UNIVERSIDADE ESTADUAL PAULISTA
"JÚLIO DE MESQUITA FILHO"

CAMPUS ARAÇATUBA
FACULDADE DE ODONTOLOGIA
FACULDADE DE MEDICINA VETERINÁRIA

CEUA - Comissão de Ética no Uso de Animais
CEUA - Ethics Committee on the Use of Animals

CERTIFICADO

Certificamos que o Projeto de Pesquisa intitulado **"Efeito da bioatividade de miniplacas de titânio texturizadas pela oxidação por plasma eletrolítico no reparo de fraturas ósseas no espectro médico-odontológico"**, Processo FOA nº 00226-2017, sob responsabilidade de Leonardo Perez Faverani apresenta um protocolo experimental de acordo com os Princípios Éticos da Experimentação Animal e sua execução foi aprovada pela CEUA em 19 de Abril de 2017.

VALIDADE DESTE CERTIFICADO: 19 de Abril de 2019.
DATA DA SUBMISSÃO DO RELATÓRIO FINAL: até 19 de Maio de 2019.

CERTIFICATE

We certify that the study entitled **"Bioactivity effect of titanium mini-plates textured by plasma elecrolytic oxidation in the bone fractures repair in the medical and dental spectrum"**, Protocol FOA nº 00226-2017, under the supervision of Leonardo Perez Faverani presents an experimental protocol in accordance with the Ethical Principles of Animal Experimentation and its implementation was approved by CEUA on April 19, 2017.

VALIDITY OF THIS CERTIFICATE: April 19, 2019.
DATE OF SUBMISSION OF THE FINAL REPORT: May 19, 2019.

Profa. Ass. Dra. Maria Gisela Laranjeira
Vice-Coordenadora da CEUA
CEUA Coordinator

CEUA - Comissão de Ética no Uso de Animais
Faculdade de Odontologia de Araçatuba
Faculdade de Medicina Veterinária de Araçatuba
Rua José Bonifácio, 1193 – Vila Mendonça - CEP: 16015-050 – ARAÇATUBA – SP
Fone (18) 3636-3234 Email CEUA: ceua@foa.unesp.br

ANEXO B - This Manuscript is already published in the “Materials Science & Engineering C” Journal

MOMESSO, Gustavo Antonio Correa et al. Miniplates coated by plasma electrolytic oxidation improve bone healing of simulated femoral fractures on low bone mineral density rats. **Materials Science and Engineering: C**, v. 120, p. 111775.

DOI: 10.1016/j.msec.2020.111775